Momentum Autocorrelation Functions and Energy Transport in Harmonic Crystals Containing Isotopic Defects

ROBERT J. RUBIN
National Bureau of Standards, Washington, D. C.
(Received 25 March 1963)

The effect of isotopic defects on the decay of the momentum autocorrelation function and on the transport of energy in a harmonic crystal is investigated. A spectral representation is obtained for the classical momentum autocorrelation function of particle j, $\rho_{jj}(t)$. The spectral density is directly related to the normal mode frequency spectrum of the crystal. The recent investigations of $\rho_{jj}(t)$ in a perfect one-dimensional crystal and a one-defect one-dimensional crystal are discussed as special cases of this general Wiener-Khinchin formula. The quantum mechanical momentum autocorrelation function of the defect particle in a one-defect crystal is treated in detail for the case in which the defect particle is very heavy. The explicit results obtained are of interest in the theory of Brownian motion. A formal relation expressing the average momentum autocorrelation function in an isotopically disordered crystal as the cosine transform of the frequency spectrum of the crystal is derived. The energy transport property is studied in terms of $\langle p^2[j,t]\rangle$, the time-dependent ensemble average dispersion of the momentum of lattice particle j when the crystal is divided initially into two regions characterized by different temperatures. A simple identity is derived, which expresses $\langle p^2[j,t]\rangle$ in terms of the solution of a particular initial value problem of the crystal lattice equations of motion. The local temperature at lattice site j, which is related to the momentum dispersion by means of the definition $\langle p^2[j,t]\rangle = M_j k_B T[j,t]$, is determined analytically in the case of the perfect and the one-defect one-dimensional crystals. The local temperature is determined numerically with the aid of an IBM-7090 computer for five isotopically disordered 100-particle one-dimensional crystals.

INTRODUCTION

THE purpose of this paper is to unify and extend the investigation of the effect of isotopic impurities on the statistical dynamical properties of harmonic crystal lattices. The crystal model considered is a perfect periodic lattice in which one or more of the lattice particles has a mass M which is different from the mass m of the remainder of the lattice particles. The forces between particles are linear in their relative displacements. Two problems are considered in detail. The first is concerned with the effect of isotopic impurities on the rate of decay of the classical and the quantum mechanical momentum autocorrelation function in a crystal characterized by a uniform temperature. The second problem is concerned with the effect of isotopic impurities on the transport of energy in a lattice which is characterized by an initial nonuniform temperature distribution. The former problem, which deals with fluctuations in an equilibrium ensemble, has received a great deal of attention recently[1–6]; the latter problem has not. Section A of this paper is devoted to the study of the momentum autocorrelation function and Sec. B to the energy transport problem. In Sec. A, a spectral representation of the momentum autocorrelation function is obtained for a canonical ensemble. In such an ensemble, the momentum of a lattice particle is a stationary Gaussian random variable and the spectral representation is a version of the Wiener-Khinchin relation between an autocorrelation function and its spectral density. In the present application, the spectral density is directly related to the normal mode frequency distribution of the lattice. In Sec. A1 the recent investigations of the classical momentum autocorrelation function in a perfect one-dimensional crystal[2,7–9] and a one-defect crystal[1–6] are discussed as special cases of the general Wiener-Khinchin formula. A formal relation between the average momentum autocorrelation function in an isotopically disordered crystal and the frequency spectrum of the crystal is obtained in Sec. A2. The quantum mechanical momentum autocorrelation function of a very heavy defect particle in an otherwise perfect one-dimensional crystal is treated in Sec. A3. The results in this section are of special interest in the theory of Brownian motion.

In Sec. B a particular energy transport problem is treated. Except for the familiar result that the thermal resistance of a harmonic crystal is zero, very little is known about the energy transport properties of such systems. The purpose of Sec. B is to formulate and to study in detail an energy transport property of a one-dimensional harmonic crystal and compare the results obtained for (1) the perfect crystal, (2) the crystal containing one isotope defect, and (3) the isotopically disordered crystal. The energy transport property is defined for a spatially nonuniform ensemble. The nonuniform ensemble is prepared by dividing the crystal lattice into two regions and clamping the particles in the surface between the two regions in

[1] R. J. Rubin, in *Proceedings of the International Symposium on Transport Processes in Statistical Mechanics, August, 1956*, edited by I. Prigogine (Interscience Publishers, Inc., New York, 1958), p. 155.
[2] P. C. Hemmer, thesis, Trondheim, Norway, 1959.
[3] R. J. Rubin, J. Math. Phys. **1**, 309 (1960).
[4] R. J. Rubin, J. Math. Phys. **2**, 373 (1961).
[5] R. E. Turner, Physica **26**, 269 (1960).
[6] S. Kashiwamura, Progr. Theoret. Phys. (Kyoto) **26**, 568 (1961); **27**, 571 (1962).
[7] G. Klein and I. Prigogine, Physica **19**, 1053 (1953).
[8] P. Mazur and E. W. Montroll, J. Math. Phys. **1**, 70 (1960).
[9] L. S. Garcia-Colin, Technical Note AFOSR-TM-60-466, 1960, Institute for Fluid Dynamics and Applied Mathematics, University of Maryland (unpublished).

their equilibrium positions so that no dynamical disturbance in one region can be communicated to the other. The two isolated regions are characterized by different canonical distributions of coordinates and momenta, i.e., the temperatures in the two regions are different. In such an ensemble, when the clamped surface particles are released, the momentum of each particle is a nonstationary Gaussian random variable. Thus, the momentum distribution function for a lattice particle is a simple Gaussian function; and we identify the time-dependent dispersion in the momentum of the particle with a local temperature.

A formal expression is derived for the time-dependent dispersion of the momentum of a lattice particle which is valid for a one-, two-, or three-dimensional harmonic crystal. The associated local temperature in the middle of the hot region of the lattice is studied analytically in the case of the perfect one-dimensional lattice in Sec. B1 and in the case of the one-defect one-dimensional lattice in Sec. B2. In Sec. B3 it is studied numerically with the aid of an IBM-7090 computer for several isotopically disordered one-dimensional crystals consisting of 100 particles, 50 of mass m_1 and 50 of mass m_2. In all three cases it is clear that energy propagates at the speed of sound, a result which is related to the infinite thermal conductivity of the crystals. However, the tails of the temperature-time curves are significantly different in the three cases.

Formal Solution of Classical and Quantum Mechanical Equations of Motion

We now obtain a formal solution of the classical and quantum mechanical equations of motion of a lattice of harmonically coupled particles which is used in Secs. A and B. The solution of the classical equations of motion expresses the momenta (or positions) of the lattice particles as time-dependent linear combinations of initial normal coordinate positions and momenta. The solution of the quantum mechanical equations of motion in the Heisenberg representation can be obtained from the classical solution by replacing the normal coordinate positions and momenta by their operator equivalents.[10]

The kinetic and potential energy quadratic forms for a harmonic crystal lattice can be written most conveniently in matrix notation as

$$\tfrac{1}{2}\dot{\mathbf{x}}^T\mathbf{M}\dot{\mathbf{x}} \quad \text{and} \quad \tfrac{1}{2}\mathbf{x}^T\mathbf{V}\mathbf{x},$$

respectively, where $\mathbf{M}$ is a diagonal matrix whose ith diagonal element M_i is the mass of the particle at lattice site i (particle i). $\mathbf{V}$ is the positive semidefinite potential energy matrix, and $\mathbf{x}$ and $\dot{\mathbf{x}}$ are column vectors whose ith components $x[i,t]$ and $\dot{x}[i,t]$ are, respectively, the displacement from equilibrium and the velocity of particle i in a given lattice direction. The superscript T denotes the transpose of a matrix. The classical equations of motion in this notation are

$$\mathbf{M}\mathbf{x}_{tt}=-\mathbf{V}\mathbf{x}. \tag{1}$$

To solve Eq. (1), introduce the vector $\mathbf{y}=\mathbf{M}^{1/2}\mathbf{x}$, and obtain $\mathbf{y}_{tt}=-\mathbf{W}\mathbf{y}$, where $\mathbf{W}=\mathbf{M}^{-1/2}\mathbf{V}\mathbf{M}^{-1/2}$. Then define the new vector $\mathbf{Q}=\mathbf{S}^T\mathbf{y}$ where the jth column of $\mathbf{S}$ is the jth normalized eigenvector of the symmetric matrix $\mathbf{W}$ associated with the frequency ω_j. [$\mathbf{S}$ is an orthogonal matrix and $\sum_j S_{jk}^2=\sum_k S_{jk}^2=1$.] The equation of motion in the new variables is diagonal in form

$$\mathbf{Q}_{tt}=-\boldsymbol{\Omega}^2\mathbf{Q}, \tag{2}$$

where the jth equation of motion is $\ddot{Q}[j,t]=-\omega_j^2Q[j,t]$. The general solution of Eq. (2) is

$$\mathbf{Q}(t)=\boldsymbol{\Omega}^{-1}\sin(\boldsymbol{\Omega}t)\mathbf{P}(0)+\cos(\boldsymbol{\Omega}t)\mathbf{Q}(0) \tag{3}$$

and

$$\mathbf{P}(t)=\cos(\boldsymbol{\Omega}t)\mathbf{P}(0)-\boldsymbol{\Omega}\sin(\boldsymbol{\Omega}t)\mathbf{Q}(0), \tag{4}$$

where $\mathbf{P}(t)=\mathbf{Q}_t(t)$ and the matrix functions $\sin(\boldsymbol{\Omega}t)$ and $\cos(\boldsymbol{\Omega}t)$ are

$$\sum_{n=0}^{\infty}\frac{(-1)^nt^{2n+1}}{(2n+1)!}\boldsymbol{\Omega}^{2n+1} \quad \text{and} \quad \sum_{n=0}^{\infty}\frac{(-1)^nt^{2n}}{(2n)!}\boldsymbol{\Omega}^{2n},$$

respectively. Consequently, the general solution of Eq. (1) is

$$\mathbf{x}(t)=\mathbf{M}^{-1/2}\mathbf{S}\boldsymbol{\Omega}^{-1}\sin(\boldsymbol{\Omega}t)\mathbf{P}(0)+\mathbf{M}^{-1/2}\mathbf{S}\cos(\boldsymbol{\Omega}t)\mathbf{Q}(0) \tag{5}$$

and

$$\mathbf{p}(t)=\mathbf{M}^{1/2}\mathbf{S}\cos(\boldsymbol{\Omega}t)\mathbf{P}(0)-\mathbf{M}^{1/2}\mathbf{S}\boldsymbol{\Omega}\sin(\boldsymbol{\Omega}t)\mathbf{Q}(0), \tag{6}$$

where the particle momenta are represented by $\mathbf{p}(t)=\mathbf{M}\dot{\mathbf{x}}(t)$.

The corresponding solutions of the Heisenberg form of the quantum mechanical equations of motion can be obtained very simply from the classical solutions in Eqs. (5) and (6). Consider the case of a harmonic oscillator with the Hamiltonian $\frac{1}{2}(P^2+\omega^2Q^2)$. The Heisenberg equations of motion for the operators $\mathfrak{Q}$ and $\mathfrak{P}$ are

$$\mathfrak{Q}_t=[\mathfrak{Q},\mathfrak{H}]=\mathfrak{P}$$
$$\mathfrak{P}_t=[\mathfrak{P},\mathfrak{H}]=-\omega^2\mathfrak{Q},$$

where $[\mathfrak{Q},\mathfrak{H}]$ denotes the commutator $-(i/\hbar)(\mathfrak{Q}\mathfrak{H}-\mathfrak{H}\mathfrak{Q})$. Due to the special commutation properties of $\mathfrak{P}$ and $\mathfrak{Q}$ with the Hamiltonian $\mathfrak{H}$, the Heisenberg equations of motion are identical with the classical Hamiltonian equations of motion of the oscillator. Consequently, corresponding to the classical solution in terms of the initial values $Q(0)$ and $P(0)$,

$$Q(t)=\cos\omega tQ(0)+\omega^{-1}\sin\omega tP(0)$$
$$P(t)=-\omega\sin\omega tQ(0)+\cos\omega tP(0),$$

one can write the quantum mechanical solution[10] in terms of the initial values of the operators $\mathfrak{Q}(0)$ and

[10] A. Messiah, *Quantum Mechanics* (Interscience Publishers, Inc., New York, 1961), Vol. 1, Chap. 12.

$\mathfrak{P}(0)$,

$$\mathfrak{Q}(t)=\cos\omega t\mathfrak{Q}(0)+\omega^{-1}\sin\omega t\mathfrak{P}(0)$$
$$\mathfrak{P}(t)=-\omega\sin\omega t\mathfrak{Q}(0)+\cos\omega t\mathfrak{P}(0).$$

This correspondence is also valid for a system of coupled oscillators. Thus, the solution of the Heisenberg equations of motion for a harmonic crystal lattice can be obtained from the classical solution by a simple substitution

$$\mathfrak{x}(t)=\mathbf{M}^{-1/2}\mathbf{S}\boldsymbol{\Omega}^{-1}\sin(\boldsymbol{\Omega}t)\mathfrak{P}(0)+\mathbf{M}^{-1/2}\mathbf{S}\cos(\boldsymbol{\Omega}t)\mathfrak{Q}(0) \quad (7)$$

and

$$\mathfrak{p}(t)=\mathbf{M}^{1/2}\mathbf{S}\cos(\boldsymbol{\Omega}t)\mathfrak{P}(0)-\mathbf{M}^{1/2}\mathbf{S}\boldsymbol{\Omega}\sin(\boldsymbol{\Omega}t)\mathfrak{Q}(0), \quad (8)$$

where the components of the vectors $\mathfrak{x}(t)$, $\mathfrak{p}(t)$ and $\mathfrak{Q}(0)$, $\mathfrak{P}(0)$ are the operators associated with the corresponding classical components of $\mathbf{x}(t)$, $\mathbf{p}(t)$ and $\mathbf{Q}(0)$, $\mathbf{P}(0)$.

A. THE MOMENTUM AUTOCORRELATION FUNCTION

Time-correlation functions play a central role in the theory of Brownian motion,[11] in studies relating to irreversible behavior [2,7,8,12,13] and in the calculation of transport coefficients[14,15] in many-body systems. In view of these general theoretical connections and the intrinsic interest in the properties of harmonic lattices containing defects, many different aspects of the calculation of correlation functions in harmonic crystals have appeared in the literature recently. For example, Klein and Prigogine,[7] Mazur and Montroll,[8] Hemmer,[2] and Garcia-Colin[9] have investigated the time-dependent behavior of the momentum autocorrelation function in perfect crystals. These authors place particular emphasis on irreversible or ergodic behavior in the limit in which the number of lattice particles N is infinite. Rubin,[1,3,4] Hemmer,[2] and Turner[5] have studied the time dependence of the correlation functions of a single heavy isotope particle substituted in an otherwise perfect crystal. Kashiwamura[6] has considered the behavior of a light mass defect in an infinite, one-dimensional crystal and has noted that the momentum autocorrelation of the light isotope does not decay to zero, but is instead a periodic function of the time. In the general case of harmonically coupled systems, formal expressions for correlation functions have been obtained by Turner,[16] Magalinskii,[17] and Kogure.[18] In addition, there are several investigations of the time-dependent behavior of particle coordinates in perfect[19–21] and imperfect[22] lattices. All of these investigations are closely related. In this section we will study in some detail a formal spectral representation of the momentum autocorrelation function which has been obtained by Turner.[16] This representation serves as a convenient starting point for all of the above-mentioned work on the one-defect problem. In addition, the same representation can be used in a formal investigation of the momentum autocorrelation function of a particle in an isotopically disordered crystal, i.e., a crystal in which the two masses M and m are distributed in an aperiodic manner on the lattice sites.

Consider the general problem of calculating the ensemble average value of the product of $p[i,t]$ the momentum of particle i at time t and $p[j,t+\tau]$ the momentum of particle j at time $t+\tau$, $\langle p[i,t]p[j,t+\tau]\rangle$. The momentum of particle i expressed as a linear combination of initial conditions, is given by the ith component of $\mathbf{p}(t)$ in Eq. (6)

$$p[i,t]=\sum_j M_i^{1/2}S_{ij}\cos(\omega_j t)P[j,0]-\sum_j M_i^{1/2}S_{ij}\omega_j\sin(\omega_j t)Q[j,0].$$

In calculating the ensemble average $\langle p[i,t]p[j,t+\tau]\rangle$, it is assumed that particle coordinates and momenta are distributed in phase space as in the canonical ensemble. The equivalent expression for the canonical distribution in the phase space of the normal coordinates is

$$\mathcal{W}[\mathbf{P}(0),\mathbf{Q}(0)]=\prod_j(2\pi k_BT)^{-1/2}\exp\{-P^2[j,0]/2k_BT\}\times\prod_j(2\pi k_BT\omega_j^{-2})^{-1/2}\exp\{-\omega_j^2Q^2[j,0]/2k_BT\}. \quad (A1)$$

From this expression, it is clear that

$$\langle P[j,0]Q[k,0]\rangle=0, \quad \langle P[j,0]P[k,0]\rangle=k_BT\delta_{kj},$$

and

$$\langle Q[j,0]Q[k,0]\rangle=\omega_j^{-2}k_BT\delta_{kj},$$

where δ_{kj} is the Kronecker delta; and the expression for $\langle p[i,t]p[j,t+\tau]\rangle$ is[23]

$$\langle p[i,t]p[j,t+\tau]\rangle=M_i^{1/2}M_j^{1/2}k_BT\sum_k S_{ik}S_{jk}\{\cos(\omega_k t)\cos[\omega_k(t+\tau)]+\sin(\omega_k t)\sin[\omega_k(t+\tau)]\}$$
$$=M_i^{1/2}M_j^{1/2}k_BT\sum_k S_{ik}S_{jk}\cos(\omega_k\tau) \quad (A2)$$
$$=M_i^{1/2}M_j^{1/2}k_BT(\mathbf{S}\cos(\boldsymbol{\Omega}\tau)\mathbf{S}^T)_{ij}. \quad (A3)$$

[11] S. Chandrasekhar, Rev. Mod. Phys. **15**, 1 (1943).
[12] A. I. Khinchin, *Mathematical Foundations of Statistical Mechanics* (Dover Publications, Inc., New York, 1949), pp. 66–69. See also P. Mazur, Rend. Scuola Intern. Fis. Enrico Fermi, **10**, 283 (1959).
[13] J. Meixner, Z. Naturforsch. **16a**, 721 (1961).
[14] M. S. Green, J. Chem. Phys. **22**, 398 (1954).
[15] R. Kubo, J. Phys. Soc. Japan **12**, 570 (1957).
[16] R. E. Turner, Physica **26**, 274 (1960).
[17] V. B. Magalinskii, Zh. Eksperim. i Teor. Fiz. **36**, 1942 (1959) [translation: Soviet Phys.—JETP **9**, 381 (1959)].
[18] Y. Kogure, J. Phys. Soc. Japan **16**, 14 (1961); **17**, 36 (1962).
[19] W. R. Hamilton, Proc. Irish Academy **1**, 267 and 341 (1839); See also A. W. Conway and A. J. McConnell, *The Mathematical Papers of Sir Willian Rowan Hamilton* (Cambridge University Press, New York, 1940), Vol. 2, pp. 451–582, 599.
[20] T. H. Havelock, Phil. Mag. **19**, 160 (1910).
[21] E. Schrödinger, Ann. Physik **44**, 916 (1914).
[22] E. Teramoto and S. Takeno, Progr. Theoret. Phys. (Kyoto) **24**, 1349 (1960).
[23] Relations of this type have been obtained by Turner, Ref. 8.

The ensemble average is independent of t as it should be. For $\tau=0$, Eq. (A2) reduces to

$$\langle p[i,t]p[j,t]\rangle = M_i^{1/2}M_j^{1/2}k_BT\delta_{ij} \tag{A4}$$

because the matrix $\mathbf{S}$ is orthogonal. If we define the momentum autocorrelation function of particle i as

$$\rho_{ii}(\tau)=\langle p[i,t]p[i,t+\tau]\rangle/\langle p^2[i,t]\rangle,$$

then

$$\rho_{ii}(\tau)=\textstyle\sum_k S_{ik}^2\cos(\omega_k\tau) \tag{A5}$$

$$=[\mathbf{S}\cos(\boldsymbol{\Omega}\tau)\mathbf{S}^T]_{ii}, \tag{A6}$$

a diagonal element of the propagator matrix

$$\mathbf{S}\cos(\boldsymbol{\Omega}\tau)\mathbf{S}^T.$$

An analogous definition of the cross correlation between the momenta of particles i and j is

$$\rho_{ij}(\tau)=\langle p[i,t]p[j,t+\tau]\rangle/\langle p^2[i,t]\rangle^{1/2}\langle p^2[j,t]\rangle^{1/2}.$$

Consequently, the expression for $\rho_{ij}(\tau)$, which is

$$\rho_{ij}(\tau)=[\mathbf{S}\cos(\boldsymbol{\Omega}\tau)\mathbf{S}^T]_{ij}, \tag{A7}$$

is symmetric in the particle labels i and j, i.e.,

$$\rho_{ij}(\tau)=\rho_{ji}(\tau).$$

Expressions for $\langle x[i,t]x[j,t+\tau]\rangle$ and $\langle x[i,t]p[j,t+\tau]\rangle$, which are analogs of the cross correlations in particle momenta, can be obtained in an identical manner.

A second interpretation can be given to Eq. (A5) due to the linearity of the equations of motion. For the special initial condition in which

$$\mathbf{x}(0)=\mathbf{0} \quad \text{and} \quad \mathbf{p}(0)=\boldsymbol{\Delta}_i, \tag{A8}$$

where all components of $\boldsymbol{\Delta}_i$ are zero except the ith component which is equal to unity, we denote the solution of the equations of motion by $\mathbf{p}(\leftarrow i,\tau)$ and $\mathbf{x}(\leftarrow i,\tau)$. It follows from Eqs. (5) and (6) that for this special initial condition $\mathbf{Q}(0)=\mathbf{0}$ and $\mathbf{P}(0)=\mathbf{S}^T\mathbf{M}^{-1/2}\boldsymbol{\Delta}_i$. The expression for $\mathbf{p}(\leftarrow i,\tau)$, the set of momenta of the lattice particles for the special initial conditions Eq. (A8), is then

$$\mathbf{p}(\leftarrow i,\tau)=\mathbf{M}^{1/2}\mathbf{S}\cos(\boldsymbol{\Omega}\tau)\mathbf{S}^T\mathbf{M}^{-1/2}\boldsymbol{\Delta}_i. \tag{A9}$$

The ith component of $\mathbf{p}(\leftarrow i,\tau)$ is

$$p[i\leftarrow i,\tau]=\rho_{ii}(\tau),$$

the momentum autocorrelation function of particle i. This identity between a dynamical and a statistical quantity for an arbitrary mass distribution and lattice structure is a generalization of a result obtained in the case of a simple cubic lattice containing a single isotopic impurity.[3,4]

There is a general dynamical reciprocity relation which is implicitly contained in Eq. (A9) and which was noted in the special case of the single defect problem.[3,4] This relation between $p[j\leftarrow i,\tau]$ and $p[i\leftarrow j,\tau]$ follows from the symmetry of the propagator $\mathbf{S}\cos(\boldsymbol{\Omega}\tau)\mathbf{S}^T$. It is

$$M_j^{-1}p[j\leftarrow i,\tau]=M_i^{-1}p[i\leftarrow j,\tau]. \tag{A10}$$

Similar kinds of relations are well known in the theory of electric networks and the theory of acoustics.[24]

The cross correlation $\rho_{ij}(\tau)$ which measures the average response at lattice site i resulting from an initial disturbance at site j is intimately connected with the energy transport properties of these lattice systems which are discussed in Sec. B. In the remainder of this section we first discuss the properties of the autocorrelation function $\rho_{jj}(\tau)$ for the infinite one-defect one-dimensional lattice. With these results as background, we next consider some formal properties of $\rho_{ij}(\tau)$ which are pertinent in the problem of the isotopically disordered lattice. Finally, we consider the quantum mechanical modification of $\rho_{jj}(\tau)$ and obtain some explicit results for the quantum mechanical momentum autocorrelation function of a very heavy defect particle in an infinite, one-dimensional crystal.

(A1) The One-Defect Crystal: Classical Mechanics

In this section the properties of the momentum autocorrelation function in the one-defect one-dimensional crystal are discussed from the point of view of the spectral representation Eq. (A5)

$$\rho_{jj}(t)=\textstyle\sum_k S_{jk}^2\cos(\omega_k t). \tag{A5}$$

Consider a one-dimensional crystal consisting of $2N+1$ particles with nearest neighbor forces and periodic boundary conditions. The particles are labeled from $-N$ to N, and particle 0 has a mass M which is different from the mass m of the other lattice particles. The equations of motion are

$$[m+(M-m)\delta_{0r}]\ddot{x}[r,t] = \kappa\{x[r+1,t]-2x[r,t]+x[r-1,t]\}, \quad -N\leqslant r\leqslant N \tag{A11}$$

with $x[-N-1,t]=x[N,t]$ and $x[N+1,t]=x[-N,t]$. Rather than determine the normal-mode frequencies and vectors for use in Eq. (A5), we solve the equations of motion (A11) for the initial values in Eq. (A8) by introducing the Laplace transform of the particle displacements $x[r,t]$. This procedure, which provides a direct approach to the problem of calculating the momentum autocorrelation function $\rho_{jj}(t)$ has been used[1,3,4] to determine $\rho_{00}(t)$, the autocorrelation of the defect particle. Expressions for both $\rho_{jj}(t)$, $j\neq 0$, and $\rho_{00}(t)$ are derived and are given in Eqs. (A20) and (A21). These expressions are particularly well suited to treat the limit in which the number of lattice particles approaches infinity.

Equations (A11) are solved by introducing a generating function. Multiply the equation for $\ddot{x}[r,t]$ by

[24] H. F. Olson, *Dynamical Analogies* (D. van Nostrand Co., Inc., Princeton, 1943), Chap. 10.

$(2N+1)^{-1/2}\exp[2\pi isr/(2N+1)]$ and sum the resulting set of equations to obtain

$$m\ddot{G}[s,t]+(2N+1)^{-1/2}(M-m)\ddot{x}[0,t] = -2\kappa\{1-\cos[2\pi s/(2N+1)]\}G[s,t], \quad \text{(A12)}$$

where the generating function $G[s,t]$ is

$$G[s,t]=(2N+1)^{-1/2}\sum_{r=-N}^{N}x[r,t]\exp[2\pi isr/(2N+1)].$$

Equation (A12) is to be solved for the special initial condition Eq. (A8) in which $\mathbf{x}(0)=\mathbf{0}$ or $G[s,0]=0$ and $\mathbf{p}(0)=\boldsymbol{\Delta}_j$ or $\dot{G}[s,0]=(2N+1)^{-1/2}M_j^{-1}\exp[2\pi isr/(2N+1)]$. Two cases must be treated separately, $j\neq 0$ and $j=0$. In case $j\neq 0$, $M_j=m$ and the Laplace transform of Eq. (A12) is

$$-(2N+1)^{-1/2}m^{-1}\exp[2\pi isj/(2N+1)]+\sigma^2\Gamma[s,\sigma] +\mathcal{Q}\sigma^2(2N+1)^{-1/2}\xi[0,\sigma] = -2\kappa m^{-1}\{1-\cos[2\pi s/(2N+1)]\}\Gamma[s,\sigma], \quad \text{(A13)}$$

where

$$\mathcal{Q}=m^{-1}M-1, \quad \Gamma[s,\sigma]=\int_0^\infty e^{-\sigma t}G[s,t]dt$$

and

$$\xi[r,\sigma]=\int_0^\infty e^{-\sigma t}x[r,t]dt.$$

Solving Eq. (A13) for $\Gamma[s,\sigma]$,

$$\Gamma[s,\sigma]=(2N+1)^{-1/2} \times\frac{m^{-1}\exp[2\pi isj/(2N+1)]-\mathcal{Q}\sigma^2\xi[0,\sigma]}{\sigma^2+2\kappa m^{-1}\{1-\cos[2\pi s/(2N+1)]\}}. \quad \text{(A14)}$$

Equation (A14) is an implicit equation since $\xi[0,\sigma]$ still appears on the right-hand side. However, $\xi[0,\sigma]$ can be determined by multiplying both sides of Eq. (A14) by $(2N+1)^{-1/2}$ and summing over all values of s, $-N\leqslant s\leqslant N$. The result is

$$\xi[0,\sigma]=m^{-1}\zeta[j,\sigma]-\mathcal{Q}\sigma^2\zeta[0,\sigma]\xi[0,\sigma]$$

or

$$\xi[0,\sigma]=m^{-1}\zeta[j,\sigma]\{1+\mathcal{Q}\sigma^2\zeta[0,\sigma]\}^{-1}, \quad \text{(A15)}$$

where

$$\zeta[j,\sigma]=(2N+1)^{-1} \times\sum_{s=-N}^{N}\frac{\exp\{2\pi isj/(2N+1)\}}{\sigma^2+2\kappa m^{-1}\{1-\cos[2\pi s/(2N+1)]\}}. \quad \text{(A16)}$$

The Laplace transform of the momentum of particle l, $m_l\sigma\xi[l,\sigma]$, can now be determined from Eq. (A14) by multiplying by $m_l\sigma(2N+1)^{-1/2}\exp[-2\pi isj/(2N+1)]$, and summing over all values of s,

$$m_l\sigma\xi[l,\sigma]=\frac{m_l}{m}\left\{\sigma\zeta[j-l,\sigma]-\frac{\mathcal{Q}\sigma^3\zeta[-l,\sigma]\zeta[j,\sigma]}{1+\mathcal{Q}\sigma^2\zeta[0,\sigma]}\right\}. \quad \text{(A17)}$$

An integral representation of $p[l\leftarrow j,t]$ for $j\neq 0$ is given by the standard inversion integral of the Laplace transform[25]

$$p[l\leftarrow j,t] =\frac{m_l/m}{2\pi i}\int_{\mathfrak{L}}e^{\sigma t}\left\{\sigma\zeta[j-l,\sigma]-\frac{\mathcal{Q}\sigma^3\zeta[-l,\sigma]\zeta[j,\sigma]}{1+\mathcal{Q}\sigma^2\zeta[0,\sigma]}\right\}d\sigma. \quad \text{(A18)}$$

When $j=0$, the corresponding expression is

$$p[l\leftarrow 0,t]=\frac{m_l/m}{2\pi i}\int_{\mathfrak{L}}e^{\sigma t}\frac{\sigma\zeta[-l,\sigma]}{1+\mathcal{Q}\sigma^2\zeta[0,\sigma]}d\sigma. \quad \text{(A19)}$$

$\mathfrak{L}$ is a line parallel to the imaginary σ axis and to the right of all singularities of the integrand. The momentum autocorrelation function $\rho_{jj}(t)$ is obtained by setting $l=j$ in Eq. (A18) and can be written as

$$\rho_{jj}(t)=\frac{1}{2\pi i}\int_{\mathfrak{L}}e^{\sigma t}\left\{\sigma\zeta[0,\sigma]-\frac{\mathcal{Q}\sigma^2\zeta^2[j,\sigma]/\zeta[0,\sigma]}{\mathcal{Q}\sigma+\{\sigma\zeta[0,\sigma]\}^{-1}}\right\}d\sigma. \quad \text{(A20)}$$

The corresponding expression for the defect particle is[8]

$$\rho_{00}(t)=\frac{\mathcal{Q}+1}{2\pi i}\int_{\mathfrak{L}}e^{\sigma t}[\mathcal{Q}\sigma+\{\sigma\zeta[0,\sigma]\}^{-1}]^{-1}d\sigma. \quad \text{(A21)}$$

The remainder of this section is devoted to (1) developing explicitly the relation between Eqs. (A20) and (A21) and the normal mode or spectral representation of the momentum autocorrelation function, Eq. (A5); and (2) determining the form of the spectral representation of $\rho_{00}(t)$ and $\rho_{jj}(t)$ in the limit of an infinite lattice as well as the asymptotic time dependence of $\rho_{00}(t)$ and $\rho_{jj}(t)$.

(1) *Relation Between the Laplace Transform Solutions in Eqs. (A20) and (A21) and the Spectral Representation of the Momentum Autocorrelation Function*

The equivalence between the expressions for $\rho_{00}(t)$ and $\rho_{jj}(t)$ in Eqs. (A20) and (A21) and the normal mode or spectral representation in Eq. (A5) is a necessary consequence of the uniqueness of the solutions of the crystal lattice equations of motion. This equivalence is easily exhibited in the case of the perfect crystal where $\mathcal{Q}=0$. Equations (A20) and (A21) are then identical

[25] P. M. Morse and H. Feshbach, *Methods of Theoretical Physics* (McGraw-Hill Book Company, Inc., New York, 1953), Vol. 1.

and the expression for the momentum autocorrelation function is

$$\rho_{jj}(t)=\frac{1}{2\pi i}\int_{\mathcal{L}}\sigma\zeta[0,\sigma]e^{\sigma t}d\sigma$$
$$=(2N+1)^{-1}\sum_{s=-N}^{N}\frac{1}{2\pi i}\int_{\mathcal{L}}\frac{\sigma}{\sigma^2+\omega_s{}^{(0)2}}e^{\sigma t}d\sigma$$
$$=(2N+1)^{-1}+2(2N+1)^{-1}\sum_{s=1}^{N}\cos(\omega_s{}^{(0)}t), \quad \text{(A22)}$$

where $\omega_s{}^{(0)}=2(\kappa/m)^{1/2}\sin[\pi s/(2N+1)]$, $s=1, \cdots N$. Equation (A22) has the same form as Eq. (A5) and has been obtained by Mazur and Montroll.[8] The calculation of $\rho_{jj}(t)$ in Eq. (A22) for the perfect crystal serves as a model for the calculation of $\rho_{jj}(t)$ and $\rho_{00}(t)$ for the one-defect crystal. The integrands in Eqs. (A20) and (A21) have simple poles on the imaginary σ axis arranged in symmetric pairs, $\sigma=\pm i\omega_k$. The sum of the residues of the integrand at a pair of poles, $\pm i\omega_k$, constitutes the term $S_{jk}{}^2\cos(\omega_k t)$ or $S_{0k}{}^2\cos(\omega_k t)$ in the spectral respresentation. These assertions, which are based on the fact that Eqs. (A20) and (A21) are unique solutions of the equations of motion of a conservative dynamical system, can be verified by direct examination of the integrands

$$\frac{1}{\mathcal{Q}\sigma+\{\sigma\zeta[0,\sigma]\}^{-1}} \quad \text{and} \quad \sigma\zeta[0,\sigma]-\frac{\mathcal{Q}\sigma^2\zeta^2[j,\sigma]/\zeta[0,\sigma]}{\mathcal{Q}\sigma+\{\sigma\zeta[0,\sigma]\}^{-1}}. \quad \text{(A23)}$$

The problem of locating the poles of the expressions in Eq. (A23) is equivalent to the problem of determining the vibration frequencies of locally perturbed systems. This last problem has been discussed extensively by Lifschitz,[26] Lax,[27] Koster and Slater,[28] and Montroll and Potts.[29] In the perfect crystal, there are N doubly degenerate normal-mode frequencies and one zero-frequency mode. In the case of the one-defect crystal, Lifschitz[26] and Montroll and Potts[29] have shown that aside from the zero-frequency mode, each pair of degenerate modes splits. As a result, two distinct groups of N normal modes are formed. In the first group of N normal modes, the amplitude of the defect particle in each mode is zero, and the associated normal-mode frequencies are the unperturbed perfect-crystal frequencies $\omega_s{}^{(0)}$, $s=1, \cdots, N$. This group of frequencies corresponds to the poles of $\sigma\zeta[0,\sigma]$ and $\sigma^2\zeta^2[j,\sigma]/\zeta[0,\sigma]$ in the integrand for $\rho_{jj}(t)$ in Eq. (A20). It is noteworthy that these poles are absent in the integral representation for $\rho_{00}(t)$, Eq. (A21), because this group of normal modes is orthogonal to the special initial condition $\mathbf{x}(0)=\mathbf{0}$, $\mathbf{p}(0)=\boldsymbol{\Delta}_0$.

[26] I. M. Lifschitz, Suppl. Nuovo Cimento **3**, 716 (1956).
[27] M. Lax, Phys. Rev. **94**, 1391 (1954).
[28] G. F. Koster and J. C. Slater, Phys. Rev. **95**, 1167 (1954).
[29] E. W. Montroll and R. B. Potts, Phys. Rev. **100**, 525 (1955).

In the second group of N normal modes, the amplitude of the defect particle is different from zero. The associated perturbed frequencies are either all increased or all decreased depending upon whether the mass of the defect particle is, respectively, greater or less than the mass of the other particles.[30] The maximum possible frequency shifts are all limited by the spacing of the unperturbed frequencies, except for the maximum frequency in the light mass case ($\mathcal{Q}<0$). These properties of the perturbed frequencies can be verified by comparing the location of the poles of $[\mathcal{Q}\sigma+\{\sigma\zeta[0,\sigma]\}^{-1}]^{-1}$ with the location of the poles of $\sigma\zeta[0,\sigma]$. In the limit as the number of lattice particles approaches infinity, a continuous band of frequencies is formed with the same limiting frequency distribution $g^{(0)}(\omega)$ as that of the perfect crystal. In addition, in the light-mass case, the maximum frequency mentioned above persists as an isolated or discrete point whose separation from the band is proportional[29] to $2(\kappa/m)^{1/2}[(1-\mathcal{Q}^2)^{-1/2}-1]$. The normal mode of vibration associated with this isolated frequency is called a "localized" mode because the amplitudes of the motion of the lattice particles decrease rapidly with increasing distance from the light-defect particle. This behavior can be understood physically in terms of the band pass characteristics of the perfect crystal when regarded as a mechanical filter.[31] The frequency associated with the light particle is greater than the band maximum. Any attempt to propagate waves through the crystal with a frequency higher than the band maximum results in a rapid attenuation of the impressed disturbance with increasing distance from the point of application. Thus, the light impurity behaves very much like a self-sustaining high-frequency disturbance. Recalling that the weight of the jth normal mode in the momentum autocorrelation function of the defect particle [or the special initial condition Eq. (A8)] is proportional to $S_{0j}{}^2$, then it can be anticipated that the localized mode will be heavily weighted. In fact, there is a large periodic component in $\rho_{00}(t)$ even in the limit $N=\infty$.[6,22]

(2) *Spectral Representation and Asymptotic Time-Dependence of $\rho_{00}(t)$ and $\rho_{jj}(t)$ in the Limit of an Infinite Crystal*

In the discussion of the explicit relation between the integral representation for $\rho_{jj}(t)$ in Eq. (A20) and the spectral representation, the central problem is the location of the poles of the integrand. In the case of the factor $[\mathcal{Q}\sigma+\{\sigma\zeta[0,\sigma]\}^{-1}]^{-1}$, the problem of the location of the poles involves the solution of a transcendental equation. This difficulty can be circumvented by

[30] Lord Rayleigh, *Theory of Sound* (Dover Publications, Inc., New York, 1945), Vol. 1, pp. 119–122. Rayleigh's general investigation is applied specifically to the isotope defect problem in A. A. Maradudin, P. Mazur, E. W. Montroll, and G. Weiss, Rev. Mod. Phys. **30**, 175 (1958); and in Ref. 29.
[31] L. Brillouin, *Wave Propagation in Periodic Structures* (Dover Publications, Inc., New York, 1953), p. 19.

considering the physically interesting limit in which the number of lattice particles approaches infinity. The simplification, which is obtained, is due to the fact that the limiting density of poles (frequencies) is the same as for the perfect crystal. Because the momentum autocorrelation function describes a local property of the lattice, and because signals propagate with the speed of sound, $(\kappa/m)^{1/2}$, it can be expected that there will be a negligible difference between the autocorrelation functions of the finite and infinite systems in the time interval $0\leqslant t<(2N+1)(\kappa/m)^{-1/2}$, where $(2N+1)\times(\kappa/m)^{-1/2}$ is the time required for a signal to travel completely around the finite system.[32] Thus, information about the relaxation behavior of the momentum autocorrelation in a large finite system can be obtained from the behavior of the infinite system. It should be emphasized that the expressions for $\rho_{00}(t)$ and $\rho_{jj}(t)$, which will be derived for the infinite crystal limit, follow directly from Eqs. (A20) and (A21). The purpose of the preceding discussion of the connection between the Laplace transform and spectral representations of the momentum autocorrelation function was to remove some of the mystery associated with this limit.

In the limit $N\rightarrow\infty$, the summation in the definition of $\zeta[j,\sigma]$, Eq. (A16), can be replaced by an integration,

$$\lim_{N\to\infty}\zeta[j,\sigma]$$
$$=\frac{1}{2\pi}\int_{-\pi}^{\pi}\exp(2\pi ij\theta)\{\sigma^2+2\kappa m^{-1}(1-\cos\theta)\}^{-1}d\theta$$
$$=\sigma^{-1}(\sigma^2+4\kappa m^{-1})^{-1/2}\left\{\frac{2(\kappa m^{-1})^{1/2}}{\sigma+(\sigma^2+4\kappa m^{-1})^{1/2}}\right\}^{2|j|} \quad \text{(A24)}$$

and

$$\lim_{N\to\infty}\zeta[0,\sigma]=\sigma^{-1}(\sigma^2+4\kappa m^{-1})^{-1/2}. \quad \text{(A25)}$$

Using this limiting expression for $\zeta[0,\sigma]$ in Eq. (A21), the autocorrelation function of the defect particle in an infinite crystal is

$$\rho_{00}(t)=\frac{\mathcal{Q}+1}{2\pi i}\int_{\mathcal{L}}\frac{e^{\sigma t}}{\mathcal{Q}\sigma+(\sigma^2+\omega_0^2)^{1/2}}d\sigma, \quad \text{(A26)}$$

where $\omega_0=2(\kappa m^{-1})^{1/2}$, the maximum frequency of the perfect crystal. In the limit $N\rightarrow\infty$, the poles along the imaginary axis, which correspond to the in-band vibration frequencies of the crystal, have merged. In their place, the integrand in Eq. (A26) contains two branch-point singularities, one at either end of the line segment of the imaginary σ axis over which the poles were densely distributed. If the branch-point singularities at $+i\omega_0$ and $-i\omega_0$ are connected by a cut along the imaginary axis, then the integrand in Eq. (A26) is analytic everywhere in the σ plane; and the spectral representation of the autocorrelation function can be obtained by using Cauchy's formula for the closed contour shown in Fig. 1. It follows from Cauchy's formula that the line integral along $\mathcal{L}$ is equal to the line integral $\mathcal{C}$ around the cut joining $+i\omega_0$ to $-i\omega_0$ plus the sum of the residues at the poles $\pm i\omega'$ corresponding to the localized mode frequency ω' in the light defect case ($\mathcal{Q}<0$). The value of ω' is determined from the condition

$$\mathcal{Q}\sigma+(\sigma^2+\omega_0^2)^{1/2}=0. \quad \text{(A27)}$$

It is easily verified that in case $\mathcal{Q}<0$ there are two roots of Eq. (A27), one at $\sigma=i\omega'=i\omega_0(1-\mathcal{Q}^2)^{-1/2}$ and one at $\sigma=-i\omega'=-i\omega_0(1-\mathcal{Q}^2)^{-1/2}$. The final result is

$$\rho_{00}(t)=2\pi^{-1}(\mathcal{Q}+1)\int_0^{\omega_0}\frac{(\omega_0^2-\omega^2)^{1/2}\cos(\omega t)}{(\mathcal{Q}^2-1)\omega^2+\omega_0^2}d\omega$$
$$+\epsilon(\mathcal{Q})\frac{2|\mathcal{Q}|}{1+|\mathcal{Q}|}\cos(\omega' t), \quad \text{(A28)}$$

where $\epsilon(\mathcal{Q})$ is a discontinuous factor which equals one if $\mathcal{Q}<0$ and zero if $\mathcal{Q}\geqslant 0$.

The spectral representation of $\rho_{00}(t)$ in Eq. (A28) is a special case of Eq. (A5) in the limit of an infinite one-dimensional crystal. The summation over normal modes in Eq. (A5) has been replaced by a weighted integral over normal-mode frequencies in Eq. (A28). For example, in case all masses are the same ($\mathcal{Q}=0$), $\rho_{00}(t)$ becomes

$$\rho_{00}(t)=2\pi^{-1}\int_0^{\omega_0}(\omega_0^2-\omega^2)^{-1/2}\cos(\omega t)d\omega. \quad \text{(A29)}$$

In this expression the quantity $2\pi^{-1}(\omega_0^2-\omega^2)^{-1/2}$ is the density of normal-mode frequencies $g^{(0)}(\omega)$ for the perfect one-dimensional crystal. In the general case

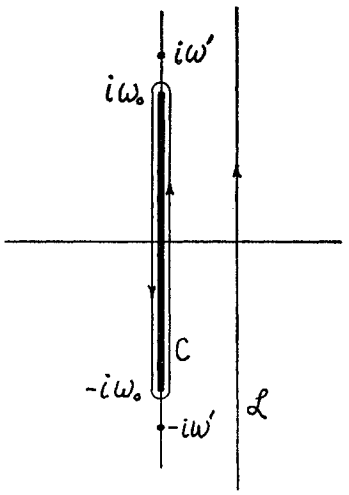

FIG. 1. σ-plane.

[32] J. C. Slater and N. H. Frank, *Mechanics* (McGraw-Hill Book Company, Inc., 1947), p. 167.

$\mathcal{Q}\neq 0$, Eq. (A28) can be written as

$$\rho_{00}(t)=\int_0^{\omega_0}\frac{(\mathcal{Q}+1)(\omega_0^2-\omega^2)}{\omega_0^2+(\mathcal{Q}^2-1)\omega^2}g^{(0)}(\omega)\cos(\omega t)d\omega + \epsilon(\mathcal{Q})\frac{2|\mathcal{Q}|}{1+|\mathcal{Q}|}\cos(\omega' t). \quad \text{(A30)}$$

Equation (A28), (A29), or (A30) has the general structure of a Wiener-Khinchin relation[33] between an autocorrelation function and its spectral density. In the present example the spectral density is

$$\frac{(\mathcal{Q}+1)(\omega_0^2-\omega^2)}{\omega_0^2+(\mathcal{Q}^2-1)\omega^2}g^{(0)}(\omega)+\epsilon(\mathcal{Q})\frac{2|\mathcal{Q}|}{1+|\mathcal{Q}|}\delta(\omega-\omega'); \quad \text{(A31)}$$

and in the special case $\mathcal{Q}=0$, the spectral density is $g^{(0)}(\omega)$. The coefficient of $g^{(0)}(\omega)$ in Eq. (A31) is the limiting form of S_{0k}^2 as $N\rightarrow\infty$ for frequencies in the band.

It is clear that the cosine transform in Eq. (A28) approaches zero as $t\rightarrow\infty$. Therefore, the autocorrelation $\rho_{00}(t)$ approaches zero if $M\geqslant m$ and it approaches $[2|\mathcal{Q}|/(1+|\mathcal{Q}|)]\cos(\omega' t)$, if $M<m$. Thus the localized mode gives rise to a persistent periodic component in the momentum autocorrelation function of the defect particle. A complete investigation of the time dependence of $\rho_{00}(t)$ has been carried out by Mazur and Montroll[8] ($\mathcal{Q}=0$), Hemmer[2] ($\mathcal{Q}=0$, $\mathcal{Q}\gg 1$), Rubin[3,4] ($\mathcal{Q}=0$, $\mathcal{Q}=1$, $\mathcal{Q}\gg 1$), and Kashiwamura[6] ($\mathcal{Q}<0$). Since $\rho_{00}(t)$ is related to a special initial value problem, there are a number of dynamical investigations which are also pertinent: Teramoto and Takeno[22] ($\mathcal{Q}<0$), and Hamilton,[19] Havelock,[20] and Schrödinger[21] ($\mathcal{Q}=0$). The latter two authors rediscovered the results obtained by Hamilton in 1839. There are only two values of $\mathcal{Q}$, $\mathcal{Q}=0$ and $\mathcal{Q}=1$, for which $\rho_{00}(t)$ and $\rho_{jj}(t)$, Eqs. (A20) and (A21), can be evaluated in closed form. The results for $\mathcal{Q}=0$ are[34]

$$\rho_{00}(t)=\rho_{jj}(t)=J_0(\omega_0 t), \quad \text{(A32)}$$

and for $\mathcal{Q}=1$ are[34]

$$\rho_{00}(t)=2(\omega_0 t)^{-1}J_1(\omega_0 t) \quad \text{(A33)}$$

and

$$\rho_{jj}(t)=J_0(\omega_0 t)-\omega_0^{-1}\frac{d}{dt}J_{4j+1}(\omega_0 t), \quad \text{(A34)}$$

where $J_n(\ )$ denotes the Bessel function of the first kind of order n. The asymptotic time dependence in these cases is different. In the perfect crystal for $t\rightarrow\infty$

$$\rho_{00}(t)\sim(2/\pi\omega_0 t)^{1/2}\cos(\omega_0 t-\pi/4). \quad \text{(A35)}$$

However, in the single defect crystal (with $\mathcal{Q}=1$), the asymptotic formula for $\rho_{00}(t)$ is

$$\rho_{00}(t)\sim\pi(2/\pi\omega_0 t)^{3/2}\sin(\omega_0 t-\pi/4). \quad \text{(A36)}$$

There are two different possible asymptotic formulas for $\rho_{jj}(t)$ when particle j is far from the defect particle 0, i.e., $j\gg 1$. The two possibilities are

$$\rho_{jj}(t)\sim(2/\pi\omega_0 t)^{1/2}\cos(\omega_0 t-\pi/4), \quad j\gg\omega_0 t\gg 1 \quad \text{(A37)}$$

and

$$\rho_{jj}(t)\sim 2^{-1}\pi[2(4j+1)^2-1](2/\pi\omega_0 t)^{3/2}\times\sin(\omega_0 t-\pi/4), \quad \omega_0 t\gg j. \quad \text{(A38)}$$

In the former case, Eq. (A37), the decay of $\rho_{jj}(t)$ is characteristic of a perfect crystal. However, after sufficient time has elapsed for the defect particle to interact with particle j, the decay law is altered to $t^{-3/2}$ as in Eq. (A38).

For any value of $\mathcal{Q}>-1$ ($0<m^{-1}M$) in the limit of an infinite system, $\rho_{00}(t)$ in Eq. (A28) always contains a decaying component. Only in the case of a light defect $-1<\mathcal{Q}<0$, is there a periodic component as well. The asymptotic time dependence of the decaying component, the cosine transform in Eq. (A28), can be obtained in a straightforward manner.[35] The result is

$$2\pi^{-1}(\mathcal{Q}+1)\int_0^{\omega_0}\frac{(\omega_0^2-\omega^2)^{1/2}}{(\mathcal{Q}^2-1)\omega^2+\omega_0^2}\cos(\omega t)d\omega \sim 2^{-1}\pi\mathcal{Q}^{-2}(\mathcal{Q}+1)(2/\pi\omega_0 t)^{3/2}\sin(\omega_0 t-\pi/4). \quad \text{(A39)}$$

Equation (A39) agrees with the result obtained by Rubin[4] in the case $\mathcal{Q}\gg 1$, and $t\rightarrow\infty$.

This variety of asymptotic decay formulas for $\rho_{jj}(t)$ in the one-dimensional one-defect lattice serves to emphasize the significant changes in time-dependent behavior accompanying the loss of the translational symmetry of the perfect crystal.

(A2) The Many-Defect Crystal: Classical Mechanics

We now consider the momentum autocorrelation function in a lattice with an arbitrary number of defects. According to Eq. (A5), we require a knowledge of the normal-mode amplitudes and frequencies in the limit as the number of particles $\mathfrak{N}$ approaches infinity. This problem can be simplified formally by introducing the average value of the momentum autocorrelation functions of all lattice particles at time t, $\bar{\rho}(t)$,

$$\bar{\rho}(t)=\mathfrak{N}^{-1}\sum_i\rho_{ii}(t) =\mathfrak{N}^{-1}\sum_j\cos(\omega_j t). \quad \text{(A40)}$$

The simpler structure of Eq. (A40) which is due to the orthogonal property of **S**, has been obtained at the expense of introducing a second average. The average

[33] M. C. Wang and G. E. Uhlenbeck, Rev. Mod. Phys. **17**, 323 (1945).

[34] A. Erdelyi, W. Magnus, F. Oberhettinger, and F. G. Tricomi, *Tables of Integral Transforms* (McGraw-Hill Book Company, Inc., New York, 1954) Vol. 1, p. 240.

[35] A. Erdelyi, *Asymptotic Expansions* (Dover Publications, Inc., New York, 1956), pp. 49–50.

autocorrelation $\bar{\rho}(t)$ no longer corresponds to a particular solution of the equations of motion. However, in the limit as $\mathfrak{N} \to \infty$, when the normal-mode frequencies form a continuum (plus possible discrete points), Eq. (A40) can be written as

$$\bar{\rho}(t) = \int_0 g(\omega) \cos(\omega t) d\omega , \qquad \text{(A41)}$$

where $g(\omega)$ is the limiting form of the frequency distribution for an arbitrary mass distribution.[36] Eq. (A41) has the Wiener-Khinchin form, and the spectral density of $\bar{\rho}(t)$ is $g(\omega)$. The only detailed information concerning $g(\omega)$ for a disordered crystal is provided in the numerical calculations of Dean[37] for one-dimensional crystals containing as many as 32 000 particles. The fine structure (numerous peaks) which he observes in $g(\omega)$ near the high frequency end of the spectrum should give rise to a complex behavior of $\bar{\rho}(t)$ [assuming that the observed form of $g(\omega)$ is maintained as $\mathfrak{N} \to \infty$].

(A3) The One-Defect Crystal: Quantum Mechanics

The time-dependent behavior of the quantum-mechanical momentum autocorrelation function of a defect particle in a one-dimensional crystal in thermal equilibrium is treated in this section. The outline of the calculation is identical with that of the classical calculation. There is, however, a difference in detail due to the noncommutativity of $\mathfrak{P}[j,0]$ and $\mathfrak{Q}[j,0]$. Our primary interest is in the case in which the defect particle is very heavy ($\mathcal{Q} \gg 1$) because it has been shown[1-4] that in the classical limit the heavy particle in a one-dimensional crystal behaves like a free Brownian particle.[11] That is, all moments of the joint position-momentum distribution function for the heavy particle, except for additive corrections of order $\mathcal{Q}^{-1}$, have the same time dependence as the corresponding moments of the distribution function for a free Brownian particle. It is shown in this section that the classical exponential form of the momentum autocorrelation function of the heavy defect persists down to temperatures far below the Debye temperature of the crystal. Eventually, however, as the temperature decreases toward zero, there is a change in the behavior of the autocorrelation function. The change becomes significant when the mean-square thermal momentum of the heavy particle ceases to be large compared to the mean square zero-point momenta of the perfect lattice normal-mode oscillators to which the heavy particle is coupled. The precise condition for Brownian-like behavior of the heavy particle is $\mathcal{Q} \gg 1$ and

$$Mk_BT \gg \tfrac{1}{2}\hbar\omega_0 m$$

or

$$\mathcal{Q} \gg \tfrac{1}{2}\Theta/T ,$$

where $\Theta = \hbar\omega_0/k_B$ is the Debye temperature. In this section, the limiting zero-temperature form of the momentum autocorrelation function of a heavy defect particle is also derived,[38] i.e., when $\mathcal{Q} \gg 1$, but $\mathcal{Q} \ll \frac{1}{2}\Theta/T$.

The momentum of particle j, expressed as a linear combination of initial independent normal-mode coordinate and momentum operators is given by the jth component of Eq. (8)

$$\mathfrak{p}[j,t] = \sum_k \{M_j^{1/2} S_{jk} \cos(\omega_k t)\mathfrak{P}[k,0] - M_j^{1/2} S_{jk}\omega_k \sin(\omega_k t)\mathfrak{Q}[k,0]\} .$$

In order to determine the quantum mechanical analog of the momentum autocorrelation function, we first form the operator corresponding to the classical quantity $p[j,t']p[j,t'+t]$. It is[39]

$$\tfrac{1}{2}\{\mathfrak{p}[j,t']\mathfrak{p}[j,t'+t] + \mathfrak{p}[j,t'+t]\mathfrak{p}[j,t']\} .$$

We then define the momentum autocorrelation function of particle j as

$$r_{jj}(t) = \langle \tfrac{1}{2}\mathfrak{p}[j,t']\mathfrak{p}[j,t'+t] + \tfrac{1}{2}\mathfrak{p}[j,t'+t]\mathfrak{p}[j,t'] \rangle / \langle \mathfrak{p}^2[j,t'] \rangle ,$$

where

$$\langle \mathfrak{p}[j,t']\mathfrak{p}[j,t'+t] \rangle = \mathrm{trace}\{\mathfrak{p}[j,t']\mathfrak{p}[j,t'+t]\mathcal{P}\}$$

and $\mathcal{P}$ is the density matrix

$$\mathcal{P} = \exp(-\mathfrak{H}/k_BT)/\mathrm{trace}\{\exp(-\mathfrak{H}/k_BT)\} .$$

$\mathfrak{H}$ is the Hamiltonian operator for the system. In the $\mathfrak{P}$, $\mathfrak{Q}$ variables, $\mathfrak{H}$ is a sum of independent oscillator Hamiltonians, and $\mathcal{P}$ is a product of independent factors

$$\mathcal{P} = \prod_j \exp(\hbar\omega_j/2k_BT)[1-\exp(-\hbar\omega_j/k_BT)]^{-1} \times \exp\{-(\mathfrak{P}^2[j,0] + \omega_j^2\mathfrak{Q}^2[j,0])/2k_BT\} = \prod_j \mathcal{P}_j .$$

Consequently, the average $\langle \mathfrak{p}[j,t']\mathfrak{p}[j,t'+t] \rangle$ can be simplified with the aid of the relations[10]:

$$\mathrm{tr}\{\mathfrak{P}[j,0]\mathfrak{P}[k,0]\mathcal{P}\} = \delta_{jk}\tfrac{1}{2}\hbar\omega_k \coth(\hbar\omega_k/2k_BT) ,$$

$$\mathrm{tr}\{\mathfrak{Q}[j,0]\mathfrak{Q}[k,0]\mathcal{P}\} = \delta_{jk}\tfrac{1}{2}\hbar\omega_k^{-1} \coth(\hbar\omega_k/2k_BT) ,$$

[36] This general result is stated in J. Hori, J. Math. Phys. **3**, 382 (1962). Hori attributes the result to Teramoto and Takeno, Ref. 22; but these latter authors treat one- and two-defect lattices only.

[37] P. Dean, Proc. Roy. Soc. (London) **254**, 507 (1960).

[38] A preliminary account of this calculation was given in R. J. Rubin, Bull. Am. Phys. Soc. **7**, 16 (1962).

[39] There have been a number of investigations of the uniqueness properties of different prescriptions for associating operators with classical dynamical variables, see J. R. Shewell, Am. J. Phys. **27**, 16 (1959). Since the operator associated with $p[j,t']p[j,t'+t]$ only involves products of the form $\mathfrak{P}[j,0]\mathfrak{P}[k,0]$, $\mathfrak{P}[j,0]\mathfrak{Q}[k,0]$ and $\mathfrak{Q}[j,0]\mathfrak{Q}[k,0]$ and since the prescriptions are unique for these simple products, we will not consider this question any further.

and

$$\mathrm{tr}\{\mathfrak{Q}[j,0]\mathfrak{P}[k,0]\mathcal{P}\}=\delta_{jk}\tfrac{1}{2}i\hbar$$
$$=-\mathrm{tr}\{\mathfrak{P}[k,0]\mathfrak{Q}[j,0]\mathcal{P}\}.$$

The expression for $\langle\mathfrak{p}[j,t']\mathfrak{p}[j,t'+t]\rangle$ is

$$\langle\mathfrak{p}[j,t']\mathfrak{p}[j,t'+t]\rangle$$
$$=\sum_k M_j S_{jk}^2\{[\cos(\omega_k t')\cos\{\omega_k(t'+t)\}+\sin(\omega_k t')$$
$$\times\sin\{\omega_k(t'+t)\}]\tfrac{1}{2}\hbar\omega_k\coth(\hbar\omega_k/2k_BT)$$
$$-\tfrac{1}{2}i\hbar\omega_k[\sin(\omega_k t')\cos\{\omega_k(t'+t)\}$$
$$-\cos(\omega_k t')\sin\{\omega_k(t'+t)\}]\}$$
$$=M_j\sum_k\tfrac{1}{2}\hbar\omega_k S_{jk}^2\{\coth(\hbar\omega_k/2k_BT)$$
$$\times\cos(\omega_k t)+i\sin(\omega_k t)\}. \quad \text{(A42)}$$

This expression, Eq. (A42), is independent of t'; and the imaginary part of $\langle\mathfrak{p}[j,t']\mathfrak{p}[j,t'+t]\rangle$ is an odd function of the time displacement t. Thus, a similar calculation of the trace of $\langle\mathfrak{p}[j,t'+t]\mathfrak{p}[j,t']\rangle$ leads to the result

$$\langle\mathfrak{p}[j,t'+t]\mathfrak{p}[j,t']\rangle=\langle\mathfrak{p}[j,t']\mathfrak{p}[j,t'+t]\rangle^*.$$

where * denotes the complex conjugate. Consequently, the quantum mechanical momentum autocorrelation function of particle j is

$$r_{jj}(t)=\mathrm{Re}\{\langle\mathfrak{p}[j,t']\mathfrak{p}[j,t'+t]\rangle\}/\langle\mathfrak{p}^2[j,t']\rangle, \quad \text{(A43)}$$

where Re{ } denotes the real part. The result for $r_{jj}(t)$ in Eqs. (A42) and (A43) is a generalization of the perfect lattice result of Mazur and Montroll.[8]

The discussion of the time dependence of the quantum mechanical momentum autocorrelation function $r_{jj}(t)$ will be limited to the system studied classically in Sec. A1, namely, a one-dimensional lattice [with periodic boundary conditions] containing a single isotope defect at lattice site zero. As a further restriction, we consider only the momentum autocorrelation function of the defect particle,

$$r_{00}(t)=\mathrm{Re}\{\langle\mathfrak{p}[0,t']\mathfrak{p}[0,t'+t]\rangle\}/\langle\mathfrak{p}^2[0,t']\rangle$$
$$=\sum_k\tfrac{1}{2}\hbar\omega_k S_{0k}^2\coth(\hbar\omega_k/2k_BT)$$
$$\times\cos(\omega_k t)/\sum_k\tfrac{1}{2}\hbar\omega_k S_{0k}^2\coth(\hbar\omega_k/2k_BT). \quad \text{(A44)}$$

In the classical limit where $\hbar\omega_k/2k_BT$ approaches zero [and $\frac{1}{2}\hbar\omega_k\coth(\hbar\omega_k/2k_BT)$ approaches k_BT], $r_{00}(t)$ approaches $\rho_{00}(t)$. In this limit an explicit integral representation has already been obtained for $\rho_{00}(t)$; it is given in Eq. (A21) as

$$\rho_{00}(t)=\sum_k S_{0k}^2\cos(\omega_k t)$$
$$=\frac{\mathcal{Q}+1}{2\pi i}\int_{\mathcal{L}}\frac{e^{\sigma t}}{\mathcal{Q}\sigma+\{\sigma\zeta[0,\sigma]\}^{-1}}d\sigma. \quad \text{(A21)}$$

By suitably modifying the path of integration and the integrand in Eq. (A21), an integral representation can be obtained for the more complicated sum, $\sum_k\frac{1}{2}\hbar\omega_k S_{0k}^2\times\coth(\hbar\omega_k/2k_BT)\cos(\omega_k t)$, appearing in Eq. (A44). Deform $\mathcal{L}$ into a closed curve $\mathcal{C}$, which encloses all the zeros of $\mathcal{Q}\sigma+\{\sigma\zeta[0,\sigma]\}^{-1}$ but excludes all poles of $\frac{1}{2}\hbar\sigma\cot(\hbar\sigma/2k_BT)$. Then we have the identity

$$\mathrm{Re}\{\langle\mathfrak{p}[0,t']\mathfrak{p}[0,t'+t]\rangle\}$$
$$=\sum_k M\tfrac{1}{2}\hbar\omega_k S_{0k}^2\coth(\hbar\omega_k/2k_BT)\cos(\omega_k t)$$
$$=M\frac{\mathcal{Q}+1}{2\pi i}\int_{\mathcal{C}}\frac{\frac{1}{2}\hbar\sigma\cot(\hbar\sigma/2k_BT)}{\mathcal{Q}\sigma+\{\sigma\zeta[0,\sigma]\}^{-1}}e^{\sigma t}d\sigma. \quad \text{(A45)}$$

In the limit in which the number of lattice particles approaches infinity, the procedure used to transform Eq. (A21) to (A26) and then to (A28) can be used for the integral in Eq. (A45). The limiting forms of Eq. (A45) for $N\to\infty$ are

$$\mathrm{Re}\{\langle\mathfrak{p}[0,t']\mathfrak{p}[0,t'+t]\rangle\}=M\frac{\mathcal{Q}+1}{2\pi i}\int_{\mathcal{C}}\frac{\frac{1}{2}\hbar\sigma\cot(\hbar\sigma/2k_BT)}{\mathcal{Q}\sigma+(\sigma^2+\omega_0^2)^{1/2}}e^{\sigma t}d\sigma \quad \text{(A46)}$$

and

$$=\frac{2}{\pi}M(\mathcal{Q}+1)\int_0^{\omega_0}\frac{(\omega_0^2-\omega^2)^{1/2}\frac{1}{2}\hbar\omega\coth(\hbar\omega/2k_BT)\cos(\omega t)}{(\mathcal{Q}^2-1)\omega^2+\omega_0^2}d\omega+\epsilon(\mathcal{Q})\frac{M|\mathcal{Q}|}{1+|\mathcal{Q}|}\hbar\omega'\coth(\hbar\omega'/2k_BT)\cos(\omega' t). \quad \text{(A47)}$$

In addition to the parameter $\mathcal{Q}$ which appears in the classical momentum autocorrelation function $\rho_{00}(t)$, the quantum mechanical momentum autocorrelation function $r_{00}(t)$ depends upon a second parameter as well, $\hbar\omega_0/2k_BT$. The mean-square dispersion in the momentum is given by

$$\langle\mathfrak{p}^2[0,t']\rangle$$
$$=M\pi^{-1}\hbar(\mathcal{Q}+1)\int_0^{\omega_0}\frac{(\omega_0^2-\omega^2)^{1/2}\omega\coth(\hbar\omega/2k_BT)}{(\mathcal{Q}^2-1)\omega^2+\omega_0^2}d\omega$$
$$+\epsilon(\mathcal{Q})\frac{M|\mathcal{Q}|}{1+|\mathcal{Q}|}\hbar\omega'. \quad \text{(A48)}$$

This result has been obtained recently by Maradudin, Flinn, and Ruby[40] and by Rubin.[38] We list for later use the value of trace$\{\mathfrak{p}^2[0,t']\mathcal{P}\}$ in the case $\mathcal{Q}\gg1$ when $T=0$:

$$\langle\mathfrak{p}^2[0,t']\rangle=M\pi^{-1}\hbar(\mathcal{Q}+1)\int_0^{\omega_0}\frac{\omega(\omega_0^2-\omega^2)^{1/2}}{(\mathcal{Q}^2-1)\omega^2+\omega_0^2}d\omega$$
$$\cong[\ln(2\mathcal{Q})-1]m\hbar\pi^{-1}\omega_0; \quad \text{(A49)}$$

and note that the corresponding classical value [when $\hbar\omega_0/2k_BT\ll1$] is $\langle p^2[0,t']\rangle=(\mathcal{Q}+1)mk_BT$.

[40] A. A. Maradudin, P. A. Flinn, and S. Ruby, Phys. Rev. **126**, 9 (1962).

The asymptotic time dependence of $\mathrm{Re}\{\langle \mathfrak{p}[0,t']\times\mathfrak{p}[0,t'+t]\rangle\}$ in Eq. (A46) is similar to the asymptotic time dependence of $\langle p[0,t']p[0,t'+t]\rangle$ in Eq. (A26). Rather than embark on a complete discussion of the time dependence of $\mathrm{Re}\{\langle \mathfrak{p}[0,t']\mathfrak{p}[0,t'+t]\rangle\}$ for all combinations of values of $\mathcal{Q}$ and $\hbar\omega_0/2k_BT$, we will confine our remarks to the case of a very heavy particle $\mathcal{Q}\gg 1$ and either $\mathcal{Q}\gg\frac{1}{2}\Theta/T$ or $\mathcal{Q}\ll\frac{1}{2}\Theta/T$.

$\mathcal{Q}\gg 1$ and $\mathcal{Q}\gg\frac{1}{2}\Theta/T$.

First, consider the case where the crystalline medium with which the heavy particle interacts is not too far below its Debye temperature ($T<\Theta$ but $\frac{1}{2}\Theta/T\ll\mathcal{Q}$, for example, $\mathcal{Q}=10^4$ and $T=(\Theta/20)$. The time-dependence of the momentum autocorrelation function $r_{00}(t)$ can be estimated using the integral representation for $\mathrm{Re}\{\langle \mathfrak{p}[0,t']\mathfrak{p}[0,t'+t]\rangle\}$, Eq. (A46). The expression for $r_{00}(t)$ is

$$r_{00}(t)=\langle \mathfrak{p}^2[0,t']\rangle^{-1}k_BTM\frac{\mathcal{Q}+1}{2\pi i}\int_{\mathfrak{C}}\frac{\phi z\cot(\phi z)}{\mathcal{Q}z+(z^2+1)^{1/2}}\times\exp(\omega_0 tz)dz, \quad \text{(A50)}$$

where $\phi=\hbar\omega_0/2k_BT=\frac{1}{2}\Theta/T$. In Eq. (A50) the closed path of integration includes the cut extending along the imaginary z axis between $+i$ and $-i$ but excludes all poles of $\phi z\cot(\phi z)$. The method used in estimating the integral in Eq. (A50) is essentially the same as the method used in treating the classical limit ($\phi=0$). Details of the analysis are given in Appendix I. The final result [Eq. (I.11) in Appendix I], which is identical in form with the classical result, is

$$r_{00}(t)=\exp(-\mathcal{Q}^{-1}\omega_0 t)+\delta(t), \quad \text{(A51)}$$

where $|\delta(t)|<c(\phi\ln\phi)\mathcal{Q}^{-1}$ and c is of order unity. This upper-bound estimate of the deviation of the autocorrelation function from $\exp(-\mathcal{Q}^{-1}\omega_0 t)$ in Eq. (A51) is valid for values of ϕ which are greater than $\pi/2$ but still small compared to $\mathcal{Q}$. For values of $\phi<\pi/2$, the corresponding estimate of $|\delta(t)|$ is $|\delta(t)|<c\mathcal{Q}^{-1}$; and in the classical limit, $\phi=0$, the value of c is[3] $2^{1/2}$. Thus, we have the result that the exponential behavior of the momentum autocorrelation function of the heavy particle persists, in the approximate sense of Eq. (A51), down to temperatures appreciably below the Debye temperature of the crystal.

The classical exponential behavior of the integral in Eq. (A50) is associated with a zero of the denominator $\mathcal{Q}z+(z^2+1)^{1/2}$ at $z=-(\mathcal{Q}^2-1)^{-1/2}$, which is close to the origin, but on a different sheet of the Riemann surface. As the temperature decreases, the poles of the function $\phi z\cot(\phi z)$ at $z=\pm\pi\phi^{-1}, \pm 2\pi\phi^{-1}, \cdots$ move in along the real axis toward the origin. At a sufficiently low temperature, the contribution to the integral from these poles overwhelms the contribution from the pole at $z=-(\mathcal{Q}^2-1)^{-1/2}$. The significant parameter which is involved is $\phi\mathcal{Q}^{-1}$. This parameter is the dominant factor in the estimate of $|\delta(t)|$ in Eq. (A51). So long as $\phi\mathcal{Q}^{-1}$ satisfies the condition $\phi\mathcal{Q}^{-1}\ll 1$, the exponential in Eq. (A51) is a precise approximation for $r_{00}(t)$. The physical parameters which make up the ratio $\phi\mathcal{Q}^{-1}$ can be rearranged as follows:

$$\phi\mathcal{Q}^{-1}=\frac{\frac{1}{2}m\hbar\omega_0}{Mk_BT}. \quad \text{(A52)}$$

It is seen from Eq. (A52) that the condition $\phi\mathcal{Q}^{-1}\ll 1$ for the persistence of the exponential form of the autocorrelation function is equivalent to the condition that the mean square zero-point momenta of all lattice normal-mode oscillators, $\frac{1}{2}m\hbar\omega$, are small compared to the mean-square momentum of the heavy particle, Mk_BT.

It should be pointed out that the system consisting of a heavy isotope defect in a three-dimensional crystal can be analyzed in an identical manner. The classical result[4] that the heavy particle behaves like a Brownian oscillator holds true in the quantum mechanical case down to temperatures well below the Debye temperature. The condition which must be satisfied is

$$\tfrac{1}{2}m\hbar\omega_0{}^{(3D)}/Mk_BT\ll 1,$$

where $\omega_0{}^{(3D)}$ is the maximum frequency of the three-dimensional crystal.

$\mathcal{Q}\gg 1$ and $\mathcal{Q}\ll\frac{1}{2}\Theta/T$

Next consider the zero-temperature limit of the momentum autocorrelation function in which $\phi\mathcal{Q}^{-1}\gg 1$. The expression for $r_{00}(t)$ is obtained by combining Eqs. (A47) and (A49) in the limiting case $\mathcal{Q}\gg 1$ and $T=0$ (or $\phi=\infty$)

$$r_{00}(t)=[\ln(2\mathcal{Q})-1]^{-1}\int_0^1\frac{y(1-y^2)^{1/2}}{y^2+\mathcal{Q}^{-2}}\cos(\omega_0 ty)dy. \quad \text{(A53)}$$

In Eq. (A53), the factor y in the numerator of the integrand, which is the limiting zero-temperature form of $y\cot(\phi y)$, significantly alters the classical exponential behavior of the integral. The details of the complete determination of the time dependence of the integral in Eq. (A53) are given in Appendix II. The principal unit of time which appears in the zero-temperature momentum autocorrelation function is $\mathcal{Q}\omega_0^{-1}$, the same as in the classical autocorrelation function. The expression for $r_{00}(t)$ in the time interval $0.01\mathcal{Q}\omega_0^{-1}<t<100\mathcal{Q}\omega_0^{-1}$, which is obtained in Eq. (II.11) in Appendix II, is

$$r_{00}(t)\cong\tfrac{1}{2}[\ln(2\mathcal{Q})-1]^{-1}[\exp(\mathcal{Q}^{-1}\omega_0 t)E_1(\mathcal{Q}^{-1}\omega_0 t)+\exp(-\mathcal{Q}^{-1}\omega_0 t)\mathrm{Re}\{E_1(\mathcal{Q}^{-1}\omega_0 te^{-i\pi})\}], \quad \text{(A54)}$$

where $E_1(z)=\int_z^\infty u^{-1}e^{-u}du$ is defined as real for real $z>0$. The function $r_{00}(t)$ in Eq. (A54) is plotted as a function of $\mathcal{Q}^{-1}\omega_0 t$ in Fig. 2 for the case $\mathcal{Q}=10^4$. It is

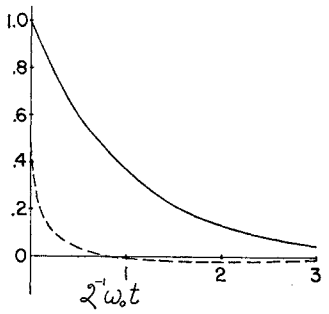

FIG. 2. The zero-temperature quantum-mechanical momentum autocorrelation function $r_{00}(t)$ is plotted as a function of $\mathcal{Q}^{-1}\omega_0 t$ for the case $\mathcal{Q}=10^4$, and is denoted by the dashed line. The classical momentum autocorrelation function

$$\exp(-\mathcal{Q}^{-1}\omega_0 t)$$

is denoted by the solid line.

represented by the dashed line. The initial value of $r_{00}(t)$ is one, by definition. The function $r_{00}(t)$ goes through the value zero in the vicinity of $t=0.875\mathcal{Q}^{-1}\omega_0 t$, assumes a minimum value, which is $-0.1558[\ln(2\mathcal{Q})-1]^{-1}$, in the vicinity of $t=1.85\mathcal{Q}\omega_0^{-1}$, and then approaches zero from below as $-[\ln(2\mathcal{Q})-1]^{-1}\times(\omega_0\mathcal{Q}^{-1}t)^{-2}$. In the transition region, where $t\gg\omega_0^{-1}$ but $t\ll\mathcal{Q}\omega_0^{-1}$, $r_{00}(t)$ is given by [see Eqs. (II.10) and (II.17) in Appendix II]

$$r_{00}(t)\cong[\ln(2\mathcal{Q})-1]^{-1}[-\gamma-\ln(\mathcal{Q}^{-1}\omega_0 t)].$$

As can be seen in Fig. 2, $r_{00}(t)$ rises very rapidly toward the value one in this range. The approximate expression for $r_{00}(t)$ in the time interval $0.1\omega_0^{-1}<t<10\omega_0^{-1}$ is obtained by combining Eqs. (II.9) and (II.14). For purposes of comparison, the classical momentum autocorrelation function $\exp(-\mathcal{Q}^{-1}\omega_0 t)$, is plotted as a solid line in Fig. 2.

B. ENERGY TRANSPORT

In this section we first formulate an energy transport problem for a harmonic crystal, and then obtain explicit solutions in the case of three one-dimensional crystals: (1) a perfect crystal, (2) a crystal containing one isotopic defect, and (3) an isotopically disordered crystal. The particular energy transport problem which we consider [41,42] has been tailored to resemble a standard initial value problem for the partial differential equation of heat conduction, i.e., a conducting medium divided into two regions with different uniform temperatures. The solution of the partial differential equation yields the temperature distribution as a function of time with the thermal conductivity of the medium as a scaling parameter for the time. In our investigation, the energy transport property is defined for a spatially nonuniform ensemble, which is prepared by dividing the crystal into two noninteracting regions. This division is accomplished by clamping the particles in the surface layer between the two regions in their equilibrium positions so that a disturbance in one region cannot be communicated to the other. If there are only nearest neighbor interactions, the layer of surface particles is one particle thick. It is assumed that the coordinates and momenta of the lattice particles in the two regions are characterized initially by independent canonical distributions with different temperatures. We consider the set of all possible initial conditions weighted according to their probability in the nonuniform ensemble. When the surface particles are released, there is, on the average, a net flow of energy from the warmer to the cooler region. Since the momentum of lattice particle j at subsequent times is a time-dependent linear combination of two independent sets of normally distributed variables (the initial particle coordinates and momenta), the probability distribution for the momentum of particle j is a normal distribution for all values of the time.[43] Taking advantage of this Gaussian property of the momentum distribution of particle j, we complete the analogy with the heat conduction problem by defining a local temperature $T[j,t]$ at lattice site j as

$$T[j,t]=(k_B M_j)^{-1}\langle p^2[j,t]\rangle, \qquad \text{(B1)}$$

where $\langle p^2[j,t]\rangle=M_j k_B T[j,t]$ is the ensemble average dispersion of the Gaussian momentum distribution of particle j at time t.

The ensemble average $\langle p^2[j,t]\rangle$ for the spatially nonuniform ensemble is determined in a straightforward manner. The final result, Eq. (B18), is similar to the result obtained for the momentum autocorrelation function in that $\langle p^2[j,t]\rangle$ is related to the particular initial value problem for the lattice equations of motion Eq. (A8). In the case of the perfect crystal Sec. B1, and the almost perfect crystal (single impurity) Sec. B2, explicit expressions for the time dependence of $\langle p^2[j,t]\rangle$ are obtained. In the case of the disordered crystal Sec. B3, we have calculated $\langle p^2[j,t]\rangle$ by integrating the equations of motion numerically for a one-dimensional system of 100 particles for the particular initial condition. The numerical results are qualitative in nature since we compare $\langle p^2[j,t]\rangle$ for a perfect monatomic crystal with $\langle p^2[j,t]\rangle$ for several isotopically disordered crystals. However, a pronounced difference in behavior between the ordered and the disordered systems is observed.

According to Eqs. (5) and (6), the initial positions and momenta are, respectively,

$$\mathbf{x}(0)=\mathbf{M}^{-1/2}\mathbf{S}\mathbf{Q}(0)$$

and

$$\mathbf{p}(0)=\mathbf{M}^{1/2}\mathbf{S}\mathbf{P}(0).$$

Consequently, the momenta at time t can be expressed in terms of $\mathbf{x}(0)$ and $\mathbf{p}(0)$ as

$$\mathbf{p}(t)=\mathbf{M}^{1/2}\mathbf{S}\cos(\boldsymbol{\Omega}t)\mathbf{S}^T\mathbf{M}^{-1/2}\mathbf{p}(0) -\mathbf{M}^{1/2}\mathbf{S}\boldsymbol{\Omega}\sin(\boldsymbol{\Omega}t)\mathbf{S}^T\mathbf{M}^{1/2}\mathbf{x}(0). \qquad \text{(B2)}$$

[41] A preliminary account of the work in this section was given in R. J. Rubin, Bull. Am. Phys. Soc. **5**, 422 (1960).

[42] E. Teramoto, Progr. Theoret. Phys. (Kyoto) **28**, 1059 (1962). Professor Teramoto considers some aspects of the perfect one-dimensional crystal energy transport problem treated in this section.

[43] T. W. Anderson, *An Introduction to Multivariate Statistical Analysis* (John Wiley & Sons, Inc., New York, 1958), Chap. 2.

Now separate the components of $\mathbf{x}(0)$ into three groups. The first group includes the coordinates of all particles in the hot region, the second group includes the coordinates of all particles in the clamped surface layer, and the third group includes the coordinates of all particles in the cold region. For an arbitrary initial state in the nonuniform ensemble, we then have

$$\mathbf{x}(0)=\begin{bmatrix}\mathbf{x}_h(0)\\ \mathbf{0}\\ \mathbf{x}_c(0)\end{bmatrix}, \tag{B3}$$

where the subscripts h and c label the coordinates of the particles in the hot and cold regions, respectively. There is a similar expression for the momenta, namely,

$$\mathbf{p}(0)=\begin{bmatrix}\mathbf{p}_h(0)\\ \mathbf{0}\\ \mathbf{p}_c(0)\end{bmatrix}. \tag{B4}$$

These expressions for $\mathbf{x}(0)$ and $\mathbf{p}(0)$ can be written in terms of the normal coordinates $\mathbf{Q}_c(0)$, $\mathbf{Q}_h(0)$ and $\mathbf{P}_c(0)$, $\mathbf{P}_h(0)$ for the two isolated regions with clamped boundaries,

$$\mathbf{x}(0)=\begin{bmatrix}\mathbf{M}_{hh}^{-1/2}\mathbf{S}_{hh}\mathbf{Q}_h(0)\\ \mathbf{0}\\ \mathbf{M}_{cc}^{-1/2}\mathbf{S}_{cc}\mathbf{Q}_c(0)\end{bmatrix} \tag{B5}$$

and

$$\mathbf{p}(0)=\begin{bmatrix}\mathbf{M}_{hh}^{1/2}\mathbf{S}_{hh}\mathbf{P}_h(0)\\ \mathbf{0}\\ \mathbf{M}_{cc}^{1/2}\mathbf{S}_{cc}\mathbf{P}_c(0)\end{bmatrix}, \tag{B6}$$

where $\mathbf{S}_{hh}$ is an orthogonal matrix whose jth column is the jth normalized eigenvector of the symmetric matrix $\mathbf{W}_{hh}=\mathbf{M}_{hh}^{-1/2}\mathbf{V}_{hh}\mathbf{M}_{hh}^{-1/2}$. The matrices $\mathbf{M}_{hh}$ and $\mathbf{V}_{hh}$ are, respectively, the mass matrix and the potential energy matrix for the hot region whose surface particles are held fixed in their equilibrium positions. The jth normalized eigenvector of $\mathbf{W}_{hh}$ is associated with the frequency $\omega_h(j)$. Thus, we have the relation $\mathbf{S}_{hh}{}^T\mathbf{W}_{hh}\mathbf{S}_{hh}=\boldsymbol{\Omega}_{hh}{}^2$, where $\boldsymbol{\Omega}_{hh}{}^2$ is a diagonal matrix whose (j,j)-element is $\omega_h{}^2(j)$, the square of the jth normal-mode frequency of region h when the surface particles are held fixed. There is a similar definition of $\mathbf{S}_{cc}$ involving $\mathbf{M}_{cc}$, $\mathbf{V}_{cc}$ and $\boldsymbol{\Omega}_{cc}{}^2$.

As already indicated, the normal coordinates and momenta for the hot region and the cold region are canonically distributed with temperatures T_h and T_c [see Eq. (A1)], respectively. The mean values are $\langle P_h[j,0]Q_h[k,0]\rangle=0$, $\langle P_h[j,0]P_h[k,0]\rangle=k_BT_h\delta_{kj}$ and $\langle Q_h[j,0]Q_h[k,0]\rangle=\omega_h{}^{-2}(j)k_BT_h\delta_{kj}$ in the classical limit, with similar relations for $Q_c[j,0]$ and $P_c[j,0]$. Clearly, there is no correlation between the h and c components. Combining Eqs. (B2), (B5), and (B6), we can express the momentum of particle j as

$$p[j,t]=\boldsymbol{\Delta}_j{}^T\left\{\boldsymbol{\gamma}(t)\begin{bmatrix}\mathbf{P}_h(0)\\ \mathbf{0}\\ \mathbf{P}_c(0)\end{bmatrix}+\dot{\boldsymbol{\gamma}}(t)\begin{bmatrix}\mathbf{Q}_h(0)\\ \mathbf{0}\\ \mathbf{Q}_c(0)\end{bmatrix}\right\},$$

where

$$\begin{aligned}\boldsymbol{\gamma}(t)&=\mathbf{M}^{1/2}\mathbf{S}\cos(\boldsymbol{\Omega}t)\mathbf{S}^T\begin{bmatrix}\mathbf{S}_{hh}&\mathbf{0}&\mathbf{0}\\ \mathbf{0}&\mathbf{0}&\mathbf{0}\\ \mathbf{0}&\mathbf{0}&\mathbf{S}_{cc}\end{bmatrix}\\ &=\mathbf{M}^{1/2}\cos(\mathbf{W}^{1/2}t)\begin{bmatrix}\mathbf{S}_{hh}&\mathbf{0}&\mathbf{0}\\ \mathbf{0}&\mathbf{0}&\mathbf{0}\\ \mathbf{0}&\mathbf{0}&\mathbf{S}_{cc}\end{bmatrix}.\end{aligned} \tag{B7}$$

The matrix $\boldsymbol{\gamma}(t)$ is a propagator matrix which governs the development in the crystal of normal-mode excitations in the hot and/or cold regions. The ensemble average $\langle p^2[j,t]\rangle$ is

$$\begin{aligned}\langle p^2[j,t]\rangle=\boldsymbol{\Delta}_j{}^T\Bigg\{&\boldsymbol{\gamma}(t)\begin{bmatrix}k_BT_h\mathbf{1}_{hh}&\mathbf{0}&\mathbf{0}\\ \mathbf{0}&\mathbf{0}&\mathbf{0}\\ \mathbf{0}&\mathbf{0}&k_BT_c\mathbf{1}_{cc}\end{bmatrix}\boldsymbol{\gamma}^T(t)\\ &+\dot{\boldsymbol{\gamma}}(t)\begin{bmatrix}k_BT_h\boldsymbol{\Omega}_{hh}{}^{-2}&\mathbf{0}&\mathbf{0}\\ \mathbf{0}&\mathbf{0}&\mathbf{0}\\ \mathbf{0}&\mathbf{0}&k_BT_c\boldsymbol{\Omega}_{cc}{}^{-2}\end{bmatrix}\dot{\boldsymbol{\gamma}}^T(t)\Bigg\}\boldsymbol{\Delta}_j.\end{aligned} \tag{B8}$$

In Eq. (B8), we can set T_c equal to zero with no loss in generality and obtain

$$\begin{aligned}&\langle p^2[j,t]\rangle\\ &=M_jk_BT_h\boldsymbol{\Delta}_j{}^T\Bigg\{\cos(\mathbf{W}^{1/2}t)\begin{bmatrix}\mathbf{1}_{hh}&\mathbf{0}&\mathbf{0}\\ \mathbf{0}&\mathbf{0}&\mathbf{0}\\ \mathbf{0}&\mathbf{0}&\mathbf{0}\end{bmatrix}\cos(\mathbf{W}^{1/2}t)\\ &\quad+\sin(\mathbf{W}^{1/2}t)\mathbf{W}^{1/2}\begin{bmatrix}\mathbf{W}_{hh}{}^{-1}&\mathbf{0}&\mathbf{0}\\ \mathbf{0}&\mathbf{0}&\mathbf{0}\\ \mathbf{0}&\mathbf{0}&\mathbf{0}\end{bmatrix}\mathbf{W}^{1/2}\sin(\mathbf{W}^{1/2}t)\Bigg\}\boldsymbol{\Delta}_j.\end{aligned} \tag{B9}$$

In order to develop the connection between Eq. (B9) and a special initial state of the lattice, we rewrite the matrix product appearing in the second term of Eq. (B9)

$$\begin{aligned}&\mathbf{W}^{1/2}\begin{bmatrix}\mathbf{W}_{hh}{}^{-1}&\mathbf{0}&\mathbf{0}\\ \mathbf{0}&\mathbf{0}&\mathbf{0}\\ \mathbf{0}&\mathbf{0}&\mathbf{0}\end{bmatrix}\mathbf{W}^{1/2}\\ &=\mathbf{W}^{-1/2}\mathbf{W}\begin{bmatrix}\mathbf{M}_{hh}{}^{1/2}\mathbf{V}_{hh}{}^{-1}\mathbf{M}_{hh}{}^{1/2}&\mathbf{0}&\mathbf{0}\\ \mathbf{0}&\mathbf{0}&\mathbf{0}\\ \mathbf{0}&\mathbf{0}&\mathbf{0}\end{bmatrix}\mathbf{W}\mathbf{W}^{-1/2}\\ &=\mathbf{W}^{-1/2}\mathbf{M}^{-1/2}\mathbf{V}\begin{bmatrix}\mathbf{V}_{hh}{}^{-1}&\mathbf{0}&\mathbf{0}\\ \mathbf{0}&\mathbf{0}&\mathbf{0}\\ \mathbf{0}&\mathbf{0}&\mathbf{0}\end{bmatrix}\mathbf{V}\mathbf{M}^{-1/2}\mathbf{W}^{-1/2}.\end{aligned} \tag{B10}$$

The matrix $\mathbf{V}$ has the form

$$\mathbf{V}=\begin{bmatrix}\mathbf{V}_{hh}&\mathbf{V}_{hs}&\mathbf{0}\\ \mathbf{V}_{sh}&\mathbf{V}_{ss}&\mathbf{V}_{sc}\\ \mathbf{0}&\mathbf{V}_{cs}&\mathbf{V}_{cc}\end{bmatrix},$$

where $\mathbf{V}_{hh}$ and $\mathbf{V}_{cc}$ are the potential energy matrices for the two regions h and c when the surface particles are held fixed in their equilibrium positions. The other elements of $\mathbf{V}$ represent interactions involving the

surface layer. The combination

$$\mathbf{V}\begin{bmatrix}\mathbf{V}_{hh}^{-1} & 0 & 0\\ 0 & 0 & 0\\ 0 & 0 & 0\end{bmatrix}\mathbf{V}$$

in Eq. (B10) reduces to

$$\mathbf{V}\begin{bmatrix}\mathbf{V}_{hh}^{-1} & 0 & 0\\ 0 & 0 & 0\\ 0 & 0 & 0\end{bmatrix}\mathbf{V}=\begin{bmatrix}\mathbf{V}_{hh} & \mathbf{V}_{hs} & 0\\ \mathbf{V}_{sh} & \mathbf{V}_{sh}\mathbf{V}_{hh}^{-1}\mathbf{V}_{hs} & 0\\ 0 & 0 & 0\end{bmatrix}. \quad \text{(B11)}$$

Combining Eqs. (B1) and (B9) and using Eqs. (B10) and (B11), the expression for $T[j,t]$ is

$$T_h^{-1}T[j,t]=\boldsymbol{\Delta}_j^T\left\{\cos(\mathbf{W}^{1/2}t)\begin{bmatrix}\mathbf{1}_{hh} & 0 & 0\\ 0 & 0 & 0\\ 0 & 0 & 0\end{bmatrix}\cos(\mathbf{W}^{1/2}t)+\mathbf{W}^{-1/2}\sin(\mathbf{W}^{1/2}t)\begin{bmatrix}\mathbf{W}_{hh} & 0 & 0\\ 0 & 0 & 0\\ 0 & 0 & 0\end{bmatrix}\mathbf{W}^{-1/2}\sin(\mathbf{W}^{1/2}t)\right\}\boldsymbol{\Delta}_j$$
$$+\boldsymbol{\Delta}_j^T\left\{\mathbf{W}^{-1/2}\sin(\mathbf{W}^{1/2}t)\mathbf{M}^{-1/2}\begin{bmatrix}0 & \mathbf{V}_{hs} & 0\\ \mathbf{V}_{sh} & \mathbf{V}_{sh}\mathbf{V}_{hh}^{-1}\mathbf{V}_{hs} & 0\\ 0 & 0 & 0\end{bmatrix}\mathbf{M}^{-1/2}\mathbf{W}^{-1/2}\sin(\mathbf{W}^{1/2}t)\right\}\boldsymbol{\Delta}_j. \quad \text{(B12)}$$

Now consider the special initial condition in which

$$\mathbf{p}(0)=M_j^{1/2}\boldsymbol{\Delta}_j \quad \text{and} \quad \mathbf{x}(0)=\mathbf{0}. \quad \text{(B13)}$$

From Eqs. (5) and (6) it is seen that $\mathbf{Q}(0)=\mathbf{0}$ and $\mathbf{P}(0)=M_j^{1/2}\mathbf{S}^T\mathbf{M}^{-1/2}\boldsymbol{\Delta}_j$; and the coordinates and momenta at time t are

$$\mathbf{x}(t)=M_j^{1/2}\mathbf{x}(\leftarrow j,t)=M_j^{1/2}\mathbf{M}^{-1/2}\mathbf{W}^{-1/2}\sin(\mathbf{W}^{1/2}t)\mathbf{M}^{-1/2}\boldsymbol{\Delta}_j$$
$$=\mathbf{M}^{-1/2}\mathbf{W}^{-1/2}\sin(\mathbf{W}^{1/2}t)\boldsymbol{\Delta}_j \quad \text{(B14)}$$

and

$$\mathbf{p}(t)=M_j^{1/2}\mathbf{p}(\leftarrow j,t)=\mathbf{M}^{1/2}\cos(\mathbf{W}^{1/2}t)\boldsymbol{\Delta}_j. \quad \text{(B15)}$$

It is readily seen that if we compute the energy in region h at time t, $\mathcal{E}[h\leftarrow j,t]$ using Eqs. (B14) and (B15) assuming that the boundary particles are clamped in their equilibrium configuration, then the result is

$$\mathcal{E}[h\leftarrow j,t]$$
$$=\tfrac{1}{2}\boldsymbol{\Delta}_j^T\left\{\cos(\mathbf{W}^{1/2}t)\begin{bmatrix}\mathbf{1}_{hh} & 0 & 0\\ 0 & 0 & 0\\ 0 & 0 & 0\end{bmatrix}\cos(\mathbf{W}^{1/2}t)\right.$$
$$+\mathbf{W}^{-1/2}\sin(\mathbf{W}^{1/2}t)\mathbf{M}^{-1/2}\begin{bmatrix}\mathbf{V}_{hh} & 0 & 0\\ 0 & 0 & 0\\ 0 & 0 & 0\end{bmatrix}$$
$$\left.\times\mathbf{M}^{-1/2}\mathbf{W}^{-1/2}\sin(\mathbf{W}^{1/2}t)\right\}\boldsymbol{\Delta}_j. \quad \text{(B16)}$$

Upon comparing Eqs. (B16) and (B12), it is seen that

$$T_h^{-1}T[j,t]=2\mathcal{E}[h\leftarrow j,t]+M_j\mathbf{x}^T(\leftarrow j,t)\mathbf{M}^{-1/2}$$
$$\times\begin{bmatrix}0 & \mathbf{V}_{hs} & 0\\ \mathbf{V}_{sh} & \mathbf{V}_{sh}\mathbf{V}_{hh}^{-1}\mathbf{V}_{hs} & 0\\ 0 & 0 & 0\end{bmatrix}\mathbf{M}^{-1/2}\mathbf{x}(\leftarrow j,t). \quad \text{(B17)}$$

In the present model, we assume that region h is convex, that the number of particles inside region h is large compared to the number of surface particles, and that particle j is located in the interior of h and far from the surface. In this case, the last term in Eq. (B17) involving surface layer particles can be neglected in comparison with $2\mathcal{E}[h\leftarrow j,t]$ provided that the elements of the matrix

$$\bar{M}\bar{\kappa}^{-1}\mathbf{M}^{-1/2}\begin{bmatrix}0 & \mathbf{V}_{hs} & 0\\ \mathbf{V}_{sh} & \mathbf{V}_{sh}\mathbf{V}_{hh}^{-1}\mathbf{V}_{hs} & 0\\ 0 & 0 & 0\end{bmatrix}\mathbf{M}^{-1/2}$$

are of order unity or less. Here $\bar{M}$ is the average mass and $\bar{\kappa}$ is the average force constant. That these matrix elements are of order unity follows from the facts that (1) the elements of $\mathbf{V}_{sh}$ and $\mathbf{V}_{hs}$ are of order $\bar{\kappa}$; (2) the diagonal elements of $\mathbf{M}^{-1/2}$ are of order $\bar{M}^{-1/2}$; and (3) the elements of $\mathbf{V}_{hh}^{-1}$ which have been obtained by Montroll and Potts[44] for a simple cubic lattice in the form of a cube, are of order $\bar{\kappa}^{-1}$. The Montroll-Potts result is

$$(\mathbf{V}_{hh}^{-1})_{\mathbf{m},\mathbf{m}'}$$
$$=\left(\frac{2}{N+1}\right)^n\sum_{s_1=1}^{N}\cdots\sum_{s_n=1}^{N}\prod_{j=1}^{n}\left\{\sin\frac{m_js_j\pi}{N+1}\sin\frac{m_j's_j\pi}{N+1}\right\}\Bigg/$$
$$2\sum_{j=1}^{n}\kappa_j\left(1-\cos\frac{s_j\pi}{N+1}\right),$$

where N is the number of particles in a cube edge and n is the dimensionality of the lattice.

Thus, the final result for $T_h^{-1}T[j,t]$, the reduced local temperature at lattice site j, when region h is initially at temperature T_h and region c is initially at temperature $T_c=0$, is

$$T_h^{-1}T[j,t]=2\mathcal{E}[h\leftarrow j,t], \quad \text{(B18)}$$

where $\mathcal{E}[h\leftarrow j,t]$ is simply the energy content of region h in the case of the special initial condition $\mathbf{x}(0)=\mathbf{0}$ and $\mathbf{p}(0)=M_j^{1/2}\boldsymbol{\Delta}_j$. The relation between $T_h^{-1}T[j,t]$ and $2\mathcal{E}[h\leftarrow j,t]$ was derived under the assumptions that the number of particles in the convex region h is large compared to the number of surface particles and that particle j is far from the surface. Clearly, under the above assumptions, the energy content of region h is insensitive to the boundary conditions

[44] E. W. Montroll and R. B. Potts, Phys. Rev. **102**, 72 (1956).

assumed in its calculation. The fixed boundary condition used in obtaining Eq. (B9) for $\langle p^2[j,t]\rangle$ was introduced only in order to treat the matrix $\mathbf{V}_{hh}^{-1}$.

In the remainder of this section the application of Eq. (B18) to the classical mechanical energy transport problem in several one-dimensional crystals is considered: a perfect crystal, a one-defect crystal, and an isotopically disordered crystal. The quantum-mechanical analog of Eq. (B18) can be obtained by replacing $k_BT_h\mathbf{1}_{hh}$ and $k_BT_c\mathbf{1}_{cc}$ by $\frac{1}{2}\hbar\boldsymbol{\Omega}_{hh}\coth(\frac{1}{2}\hbar\boldsymbol{\Omega}_{hh}/k_BT_h)$ and $\frac{1}{2}\hbar\boldsymbol{\Omega}_{cc}\coth(\frac{1}{2}\hbar\boldsymbol{\Omega}_{cc}/k_BT_c)$, respectively. However, we will not treat these modifications in this paper. We merely observe in this case that (1) there is no simple relation between $\langle p^2[j,t]\rangle$ and an initial value problem; and (2) there will be a dependence of the cooling curve on the initial temperature difference T_h-T_c when $\hbar\omega_0/k_BT_h$ is of the order of magnitude of unity, or less.

(B1) The Perfect One-Dimensional Crystal

To illustrate the general result which has been obtained for the reduced time-dependent local temperature, we will treat a perfect infinite one-dimensional crystal for which particles $-L-1$ and $L+1$ are held initially in their equilibrium positions. The portion of the crystal between $-L-1$ and $L+1$ is characterized by a canonical distribution (temperature T_h). The rest of the crystal is at $T_c=0$. In this case, as well as for the one-defect one-dimensional crystal, we obtain an explicit expression for the ensemble average dispersion of the momentum of the particle in the middle of the hot region. This dispersion, which is related to a reduced local temperature, can be determined from $\mathcal{E}[h\leftarrow 0,t]$, the energy contained between particles $-L-1$ and $L+1$ at time t for the special initial condition in the infinite lattice, $\mathbf{x}(0)=\mathbf{0}$ and $\mathbf{p}(0)=M_0^{1/2}\boldsymbol{\Delta}_0$. The position $x[l,t]$ and momentum $p[l,t]$ of particle l at time t, which are associated with the above special initial condition, were first determined by Hamilton[19] and subsequently by Havelock[20] and Schrödinger.[21] The momentum $p[l,t]$ is also obtained as a special case of Eq. (A18)

$$p[l,t]=\frac{m^{1/2}}{2\pi i}\int_{\mathfrak{L}}\sigma\zeta[-l,\sigma]e^{\sigma t}d\sigma\,, \tag{A18}$$

where in the present case $M_0=M_j=m$. In the limit $N\to\infty$, the expression for $\zeta[-l,\sigma]$, Eq. (A16), becomes

$$\zeta[-l,\sigma]=\frac{1}{2\pi}\int_{-\pi}^{\pi}e^{-il\theta}[\sigma^2+2\kappa m^{-1}(1-\cos\theta)]^{-1}d\theta \tag{B19}$$

$$=\pi^{-1}\int_{-\pi/2}^{\pi/2}e^{-2il\phi}[\sigma^2+\omega_0^2\sin^2\phi]^{-1}d\phi.$$

Substituting this last expression in Eq. (A18) and inverting the Laplace transform, one obtains

$$p[l,t]=m^{1/2}\pi^{-1}\int_{-\pi/2}^{\pi/2}e^{-2il\phi}\cos(\omega_0 t\sin\phi)d\phi$$

$$=m^{1/2}J_{2|l|}(\omega_0 t). \tag{B20}$$

The position of particle l at time t is

$$x[l,t]=m^{-1}\int_0^t p[l,s]ds$$

$$=m^{-1/2}\int_0^t J_{2|l|}(\omega_0 s)ds. \tag{B21}$$

The expression for the energy $\mathcal{E}[h\leftarrow 0,t]$ is

$$\mathcal{E}[h\leftarrow 0,t]$$
$$=\tfrac{1}{2}\sum_{l=-L}^{L}J_{2|l|}^2(\omega_0 t)$$
$$+\tfrac{1}{2}\kappa\sum_{l=-L+1}^{L}\left\{m^{-1/2}\int_0^t[J_{2|l|}(\omega_0 s)-J_{2|l-1|}(\omega_0 s)]ds\right\}^2$$
$$+\kappa m^{-1}\left\{\int_0^t J_{2L}(\omega_0 s)ds\right\}^2$$
$$=\tfrac{1}{2}J_0^2(\omega_0 t)+\sum_{l=1}^{2L}J_l^2(\omega_0 t)+\frac{1}{4}\left\{\int_0^{\omega_0 t}J_{2L}(s)ds\right\}^2. \tag{B22}$$

The last term in Eq. (B22), which is a surface energy term, is negligible in comparison with $\mathcal{E}[h\leftarrow 0,t]$. It follows directly from the properties of Bessel functions that the initial and final values of the reduced local temperature are 1 and 0, respectively. Furthermore, if the hot region consists of the entire crystal ($L=\infty$), the constant value of the temperature follows from a special case of a well-known addition formula for Bessel functions,[45]

$$J_0^2(\omega_0 t)+2\sum_{l=1}^{\infty}J_l^2(\omega_0 t)=1. \tag{B23}$$

Our principal concern in this example is to determine the time dependence of the reduced local temperature (the cooling curve) at particle 0 for the case in which L is large, but finite. It is convenient to introduce a new dimensionless time variable τ_L which is measured in units of $2L\omega_0^{-1}$, the time taken by a signal moving at the group velocity of very long waves to go from lattice site 0 to L,

$$\tau_L=t/2L\omega_0^{-1}.$$

In terms of this new time variable, the expression for

[45] W. Magnus and F. Oberhettinger, *Formulas and Theorems for the Special Functions of Mathematical Physics* (Chelsea Publishing Company, New York, 1949), p. 19.

the reduced local temperature can be written as

$$T_h^{-1}T[0,\tau_L]=J_0^2(2L\tau_L)+2\sum_{l=1}^{2L}J_l^2\left(l\frac{2L}{l}\tau_L\right). \quad \text{(B24)}$$

In evaluating the sum in Eq. (B24), we utilize a uniform asymptotic expansion of Bessel functions (with error estimates) which has been developed by Olver.[46,47] The expansion, although expressed in a complicated parametric form, ultimately leads to a remarkably simple result for the sum in Eq. (B24). Details of the analysis are given in Appendix III. The expression obtained for the reduced local temperature, which is exact except for correction terms of order $(2L)^{-1}$, is

$$T_h^{-1}T[0,\tau_L]=\begin{cases}1, \text{ if } \tau_L<1-(2L)^{-1/3}\\ (2/\pi)\sin^{-1}(1/\tau_L), \text{ if } \tau_L>1+(2L)^{-1/3}.\end{cases} \quad \text{(B25)}$$

In Eq. (B25) the reduced local temperature or mean local kinetic energy drops abruptly from its initial value as soon as signals, which originate when the boundary particles $-L-1$ and $L+1$ are released, reach the middle of the hot region. For large values of τ_L the asymptotic formula for $T_h^{-1}T[0,\tau_L]$ is

$$T_h^{-1}T[0,\tau_L]\sim 2\pi^{-1}\tau_L^{-1}. \quad \text{(B26)}$$

It will be seen in the next section that the time dependence of the result in Eq. (B26) is determined only in part by the dispersion relation between normal-mode frequency and wavelength. The time dependence of the reduced local temperature for $\tau_L\gg 1$ should be compared with the analogous result in the classical heat conduction problem[48] for the case of an infinite one-dimensional rod with the initial temperature distribution

$$T(x,0)=\begin{cases}0, & x<-L\\ T_h, & -L\leqslant x\leqslant L\\ 0, & L<x.\end{cases}$$

The reduced local temperature in the middle of the hot region in this latter case is

$$T_h^{-1}T(0,t)=(2\pi)^{-1/2}\int_{-L(2Dt)^{-1/2}}^{L(2Dt)^{-1/2}}\exp(-\tfrac{1}{2}\eta^2)d\eta,$$

where D is proportional to the thermal conductivity. For large values of the time, the expression for $T_h^{-1}T(0,t)$ reduces to

$$T_h^{-1}T(0,t)\sim\pi^{-1}L(2Dt)^{-1/2},$$

a result which is entirely different from Eq. (B26).

[46] F. W. J. Olver, Phil. Trans. Roy. Soc. **247**, 307 and 328 (1954).

[47] Explicit error estimates of the asymptotic series derived in Ref. 46 are given in F. W. J. Olver, *Tables for Bessel Functions of Moderate or Large Order*, Mathematical Tables, National Physical Laboratory (Her Majesty's Stationery Office, London, 1962), Vol. 6.

[48] A. Sommerfeld, *Partial Differential Equations in Physics* (Academic Press Inc., New York, 1949), p. 58.

(B2) The Single Defect One-Dimensional Crystal

In this section we treat the energy transport problem for the single defect, infinite, one-dimensional crystal lattice. Although the introduction of a single defect particle cannot be expected to alter the sound speed in the crystal, we find that the time dependence of the reduced local temperature can be profoundly altered for $\tau_L>1$. For purposes of illustration, we will treat two cases in which the defect particle is located at lattice site zero: the mass M of the defect particle is either $M=2m$ or $M<m$.

Case 1. The Mass of the Defect Particle at Lattice Site Zero is $M=2m$

When the mass of the defect particle is $2m$, the particle positions and momenta for the special initial condition, $\mathbf{x}(0)=\mathbf{0}$ and $\mathbf{p}(0)=(2m)^{1/2}\boldsymbol{\Delta}_0$, can be expressed in terms of Bessel functions of the first kind; and consequently, the analysis of the last section can be utilized.

The momentum of particle l corresponding to the initial condition $\mathbf{x}(0)=\mathbf{0}$ and $\mathbf{p}(0)=(2m)^{1/2}\boldsymbol{\Delta}_0$ is, according to Eq. (A19),

$$p[l,t]=(2m)^{1/2}\frac{m_l/m}{2\pi i}\int_{\mathcal{L}}\frac{\sigma\zeta[-l,\sigma]}{1+\sigma^2\zeta[0,\sigma]}e^{\sigma t}d\sigma. \quad \text{(B27)}$$

The value of $\zeta[-l,\sigma]$ can be obtained from Eq. (B19) as follows:

$$\begin{aligned}\zeta[-l,\sigma]&=\frac{1}{2\pi}\int_{-\pi}^{\pi}e^{-il\theta}[\sigma^2+2\kappa m^{-1}(1-\cos\theta)]^{-1}d\theta\\ &=\int_0^\infty\exp(-2\kappa m^{-1}u-\sigma^2u)\\ &\quad\times\left\{(2\pi)^{-1}\int_{-\pi}^{\pi}\exp(-il\theta+2u\kappa m^{-1}\cos\theta)d\theta\right\}du\\ &=\int_0^\infty\exp(-2\kappa m^{-1}u-\sigma^2u)I_{|l|}(2\kappa m^{-1}u)du\\ &=(2\kappa m^{-1})^{|l|}[(2\kappa m^{-1}+\sigma^2)^2-4\kappa^2m^{-2}]^{-1/2}\\ &\quad\times\{2\kappa m^{-1}+\sigma^2+[(2\kappa m^{-1}+\sigma^2)^2-4\kappa^2m^{-2}]^{1/2}\}^{-|l|}\end{aligned}$$

$$\zeta[-l,\sigma]=\omega_0^{2|l|}\sigma^{-1}(\sigma^2+\omega_0^2)^{-1/2}\{\sigma+(\sigma^2+\omega_0^2)^{1/2}\}^{-2|l|}, \quad \text{(B28)}$$

where $I_n(\ )$ is a modified Bessel function of order n of the first kind. The result of substituting this expres-

sion in Eq. (B27) for $p[l,t]$ is

$$p[l,t]=(2m)^{1/2}\frac{m_l/m}{2\pi i}\int_{\mathcal{L}}\frac{\omega_0^{2|l|}\exp(\sigma t)}{[\sigma+(\sigma^2+\omega_0^2)^{1/2}]^{2|l|+1}}d\sigma$$
$$=(2m)^{1/2}(m_l/m)(\omega_0 t)^{-1}(2|l|+1)J_{2|l|+1}(\omega_0 t). \quad \text{(B29)}$$

The corresponding position of particle l at time t is

$$x[l,t]=(2/m)^{1/2}(2|l|+1)\int_0^t(\omega_0 s)^{-1}J_{2|l|+1}(\omega_0 s)ds. \quad \text{(B30)}$$

The energy $\mathcal{E}[h\leftarrow 0,t]$ is

$$\mathcal{E}[h\leftarrow 0,t]$$
$$=\sum_{l=-L}^{L}\frac{m_l}{m}\frac{(2|l|+1)^2}{\omega_0^2t^2}J_{2|l|+1}^2(\omega_0 t)$$
$$+\kappa m^{-1}\sum_{l=-L}^{L}\left\{\int_0^t\left[\frac{2|l|+1}{\omega_0 s}J_{2|l|+1}(\omega_0 s)\right.\right.$$
$$\left.\left.-\frac{2|l|-1}{\omega_0 s}J_{2|l|-1}(\omega_0 s)\right]ds\right\}^2$$
$$+2\kappa m^{-1}\left\{\int_0^t\frac{2L+1}{\omega_0 s}J_{2L+1}(\omega_0 s)ds\right\}^2$$
$$=2\omega_0^{-2}t^{-2}\sum_{l=1}^{2L+1}l^2J_l^2(\omega_0 t)$$
$$+\frac{1}{2}\left\{\int_0^{\omega_0 t}(2L+1)s^{-1}J_{2L+1}(s)ds\right\}^2. \quad \text{(B31)}$$

For $L\gg 1$, the expression for the reduced local temperature is

$$T_h^{-1}T[0,\tau_L]=4\tau_L^{-2}\sum_{l=1}^{2L}(l/2L)^2J_l^2\left(l\frac{2L}{l}\tau_L\right). \quad \text{(B32)}$$

With trivial changes, the analysis of the last section can be used to obtain the following result in the limit $L\gg 1$,

$$T_h^{-1}T[0,\tau_L]$$
$$=\begin{cases}1, \text{ if } \tau_L<1-(2L)^{-1/3}\\ 4\pi^{-1}\tau_L^{-2}\displaystyle\int_0^1\frac{y^2dy}{(\tau_L^2-y^2)^{1/2}}, \text{ if } \tau_L>1+(2L)^{-1/3}\end{cases}$$

$$T_h^{-1}T[0,\tau_L]$$
$$=\begin{cases}1, \text{ if } \tau_L<1-(2L)^{-1/3}\\ 2\pi^{-1}[\sin^{-1}(1/\tau_L)-\tau_L^{-1}(1-\tau_L^{-2})^{1/2}],\\ \qquad\qquad \text{if } \tau_L>1+(2L)^{-1/3}.\end{cases} \quad \text{(B33)}$$

The reduced local temperature in the present case is plotted as a function of τ_L (solid curve) in Fig. 3 along with the reduced local temperature in the perfect crystal case (dashed curve). The asymptotic value of $T_h^{-1}T[0,\tau_L]$ when $M_0=2m$ is

$$T_h^{-1}T[0,\tau_L]\sim(4/3\pi)\tau_L^{-3}, \quad \text{for} \quad \tau_L\gg 1.$$

The τ_L^{-3} dependence of $T_h^{-1}T[0,\tau_L]$ should be expected whenever the mass of the defect particle is greater than the normal value; it is associated with the $t^{-3/2}$ dependence of the momentum found in Eqs. (A36), (A38), and (A39). Of course, if the defect particle is located far enough away from lattice site zero, perfect crystal behavior, Eq. (B25), should be observed. We next consider the case of a light defect particle in which a different type of behavior is found.

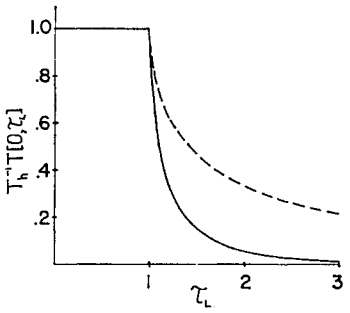

FIG. 3. The reduced local temperature in the middle of a hot region is plotted as a function of τ_L for two cases. The dashed curve corresponds to the case of the perfect crystal. The solid curve corresponds to the case in which the mass of the central particle is twice the mass of the other particles.

Case 2. The Mass of the Defect Particle at Lattice Site Zero is $M_0<m$

When the mass of particle zero is less than m, a localized mode is present. Consequently, in the calculation of the mean local temperature at lattice site zero, the position of the defect, it can be anticipated that the partial energy $\mathcal{E}[h\leftarrow 0,t]$, and therefore $T_h^{-1}T[0,t]$, will not decay to zero. This behavior results from the large localized mode component contained in the initial condition $\mathbf{x}(0)=\mathbf{0}$ and $\mathbf{p}(0)=M_0^{1/2}\boldsymbol{\Delta}_0$. The energy associated with the localized mode, which is a constant of the motion as for the other normal modes, is concentrated permanently in the vicinity of particle zero. In this section we will calculate the energy of the localized mode in the energy-transport problem when the light particle is at lattice site zero.

The momentum of particle l corresponding to the initial condition Eq. (B13) is, according to Eqs. (A19) and (B28)

$$p[l,t]=M_0^{1/2}\frac{M_l/m}{2\pi i}\int_{\mathcal{L}}\omega_0^{2|l|}[\mathcal{Q}\sigma+(\sigma^2+\omega_0^2)^{1/2}]^{-1}$$
$$\times[\sigma+(\sigma^2+\omega_0^2)^{1/2}]^{-2|l|}e^{\sigma t}d\sigma.$$

In the present case, with $\mathcal{Q}=m^{-1}M-1<0$, the localized mode component of $p[l,t]$ which comes from the isolated poles at $\sigma=\pm i\omega_0(1-\mathcal{Q}^2)^{-1/2}=\pm i\omega'$ is

$$M_0^{1/2}\frac{2(M_l/m)}{\mathcal{Q}+|\mathcal{Q}|^{-1}}(-1)^l\left(\frac{1-|\mathcal{Q}|}{1+|\mathcal{Q}|}\right)^{|l|}\cos(\omega' t). \quad \text{(B34)}$$

The coefficient of $\cos(\omega' t)$ in Eq. (B34) is proportional to the displacement of the lth particle in the localized mode and exhibits the known properties of alternation in sign and decrease with increasing $|l|$. The localized mode component in the position of particle l is

$$\frac{M_0^{1/2}(2/m)}{\mathcal{Q}+|\mathcal{Q}|^{-1}}(-1)^l\left(\frac{1-|\mathcal{Q}|}{1+|\mathcal{Q}|}\right)^{|l|}\frac{\sin(\omega' t)}{\omega'}. \quad \text{(B35)}$$

If we calculate the energy $\mathcal{E}'[h\leftarrow 0,t]$ associated with these periodic components when $L\gg 1$, we obtain the result

$$\mathcal{E}'[h\leftarrow 0,t]=|\mathcal{Q}|/(1+|\mathcal{Q}|), \quad \text{for} \quad -1<\mathcal{Q}\leqslant 0. \quad \text{(B36)}$$

Consequently, the mean local temperature at the site of the defect particle, which is defined in Eq. (B1), approaches a limiting value greater than zero as $t\rightarrow\infty$, namely, $2\mathcal{E}'[h\leftarrow 0,t]$,

$$T_h^{-1}T[0,\infty]=2|\mathcal{Q}|/(1+|\mathcal{Q}|), \quad \text{for} \quad -1<\mathcal{Q}\leqslant 0. \quad \text{(B37)}$$

(B3) Energy Transport in an Isotopically Disordered Crystal

We have shown in the preceding sections that the introduction of single isotopic defects into a harmonic crystal lattice can alter greatly the time dependence of the local temperature defined in Eq. (B1). The cases considered were extreme. Clearly, the behavior of the local temperature at a point far removed from an isotope defect will resemble that of the perfect crystal. However, an interesting question which still remains is how this local temperature will vary in a completely disordered crystal composed of equal numbers of particles of mass m_1 and m_2. In attempting to answer this question, we have resorted to a direct numerical evaluation of $\mathcal{E}[h\leftarrow 0,t]$ in Eq. (B16). Using the IBM 7090, we have solved the initial value problem,

$$\mathbf{M}\mathbf{x}_{tt}=-\mathbf{V}\mathbf{x} \quad (1)$$

with $\mathbf{x}(0)=\mathbf{0}$ and $\mathbf{p}(0)=M_0^{1/2}\boldsymbol{\Delta}_0$ and periodic boundary conditions, in a series of one-dimensional isotopically disordered 100-particle crystals in which there are 50 particles of mass m_1, and 50 particles of mass m_2. The only differences in the series of calculations lie in the order of the m_1's and m_2's along the diagonal of $\mathbf{M}$ and in the numerical value of the ratio of the particle masses m_2/m_1. Having calculated $\mathbf{x}(t)$ and $\mathbf{p}(t)$ for each of several different mass distributions, we then determined reduced local temperatures from Eq. (B18) and compared them with the corresponding reduced local temperature computed for the perfect monatomic crystal composed of particles with the harmonic mean mass $\bar{m}=2(m_1^{-1}+m_2^{-1})^{-1}$.

The method used for generating the solution of the equations of motion Eq. (1) from the initial condition $\mathbf{x}(0)=\mathbf{0}$ and $\mathbf{p}(0)=M_0^{1/2}\boldsymbol{\Delta}_0$ is an iterative one which is based on the general solution Eqs. (5) and (6),

$$\begin{aligned}\mathbf{x}(t_0)&=\mathbf{M}^{-1/2}\mathbf{S}\boldsymbol{\Omega}^{-1}\sin(\boldsymbol{\Omega}t_0)\mathbf{S}^T\mathbf{M}^{-1/2}\mathbf{p}(0)\\&\quad+\mathbf{M}^{-1/2}\mathbf{S}\cos(\boldsymbol{\Omega}t_0)\mathbf{S}^T\mathbf{M}^{1/2}\mathbf{x}(0)\\&=\mathbf{M}^{-1/2}\mathbf{W}^{-1/2}\sin(\mathbf{W}^{1/2}t_0)\mathbf{M}^{-1/2}\mathbf{p}(0)\\&\quad+\mathbf{M}^{-1/2}\cos(\mathbf{W}^{1/2}t_0)\mathbf{M}^{1/2}\mathbf{x}(0) \quad (5)\end{aligned}$$

and

$$\begin{aligned}\mathbf{p}(t_0)&=\mathbf{M}^{1/2}\cos(\mathbf{W}^{1/2}t_0)\mathbf{M}^{-1/2}\mathbf{p}(0)\\&\quad-\mathbf{M}^{1/2}\mathbf{W}^{1/2}\sin(\mathbf{W}^{1/2}t_0)\mathbf{M}^{1/2}\mathbf{x}(0), \quad (6)\end{aligned}$$

where $\mathbf{W}=\mathbf{M}^{-1/2}\mathbf{V}\mathbf{M}^{-1/2}$. The series expansions of the matrices $\cos(\mathbf{W}^{1/2}t_0)$ and $\mathbf{W}^{\pm 1/2}\sin(\mathbf{W}^{1/2}t_0)$ in Eqs. (5) and (6) involve only integer powers of the matrix $\mathbf{W}$, e.g.,

$$\cos(\mathbf{W}^{1/2}t_0)=\sum_{m=0}^{\infty}(-1)^m\frac{t_0^{2m}}{(2m)!}\mathbf{W}^m.$$

For values of t_0 of the order of $[\frac{1}{2}\kappa(m_1^{-1}+m_2^{-1})]^{-1/2}$, which is the time required for a long-wavelength disturbance to travel one lattice spacing, the first eight terms in the series expansions of the matrices $\cos(\mathbf{W}^{1/2}t_0)$ and $\mathbf{W}^{\pm 1/2}\sin(\mathbf{W}^{1/2}t_0)$ are sufficient to give values of their elements correct to eight significant figures. Thus, for a given arrangement of the masses m_1 and m_2, it is possible with the aid of the IBM 7090 to calculate the elements of the propagator matrices in Eqs. (5) and (6). Values of $\mathbf{x}(t_0)$ and $\mathbf{p}(t_0)$ can then be computed from the initial conditions. This process, when repeated n times, produces the values of $\mathbf{x}(nt_0)$ and $\mathbf{p}(nt_0)$ from which $\mathcal{E}[h\leftarrow 0,nt_0]$ can be calculated. Provision was made in the computing program for generating random mass distributions[49] consisting of equal numbers of m_1's and m_2's.

The results of the calculations for a series of five different isotopically disordered 100-particle crystals are presented in Fig. 4 for the case in which the mass ratio is $m_2/m_1=5/4$. The reduced mean local temperature at the middle of the initially hot region is plotted as a function of the time τ_L which is measured in units of the time required for sound to travel from the middle to the boundary of the hot region. The partial energies were computed for hot regions consisting of a total of 21, 31, and 51 particles ($L=10$, 15, and 25, respectively); and the curves shown in Fig. 4 are those pertaining to the case of 31 particles. For purposes of comparison we have also plotted (open circles) the corresponding cooling curve for a perfect monatomic 100-particle crystal in which the sound speed is the same as in the regular diatomic crystal composed of particles of mass m_1 and m_2, namely, one in which the force constant to mass ratio is $\kappa/\bar{m}$, where $\bar{m}$ is the harmonic mean of m_1 and m_2, $\bar{m}=2(m_1^{-1}+m_2^{-1})^{-1}$. All of the disordered crystal cooling curves lie above the one for

[49] O. Taussky and J. Todd, in *Symposium on Monte Carlo Methods*, edited by H. A. Meyer (John Wiley & Sons, Inc., New York, 1956). These authors describe the congruential multiplicative method used in our calculations.

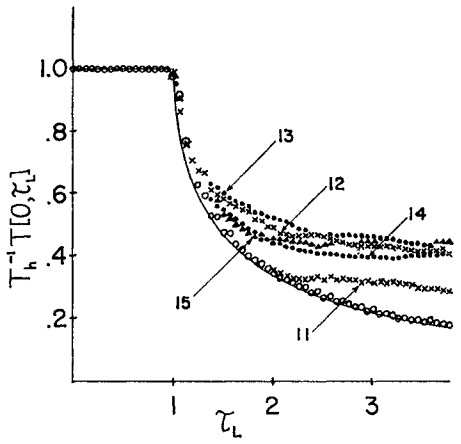

FIG. 4. The reduced local temperature in the middle of a hot region is plotted as a function of τ_L for five different isotopically disordered 100-particle crystals containing 50 particles of mass m_1 and 50 of mass $(5/4)m_1$. Different isotope arrangements are denoted by the number used in their generation, e.g., 11, 12, $\cdots$, 15. For the cases shown, L is 15. The corresponding reduced local temperature is plotted for a perfect crystal (open circles) consisting of 100 particles with the harmonic mean mass $\bar{m}=(10/9)m_1$. The solid curve represents the analytic result for the perfect crystal, Eq. (B25).

the perfect crystal. The cooling curve for the perfect crystal for $L\gg1$, Eq. (B25), is shown as a solid curve in Fig. 4, and is remarkably close to the computed values in the present case, $L=15$ (open circles). It should be emphasized that for the range of τ_L covered in Fig. 4 the shapes of all the cooling curves are independent of the nature of the crystal boundary conditions, or, what is equivalent, independent of the finite size of the system. This statement is based on the fact that the minimum time required for a sound signal originating in the center of a 31-particle hot region of a 100-particle crystal and traveling through one side of the hot region to reach the other side (or be reflected back from particle number 50) is $\tau_L=5\frac{2}{3}$, and the maximum τ_L in Fig. 4 is less than 4. We have tested the accuracy of the procedure used for integrating the equations of motion by reversing all particle velocities at $\tau_L=2$. It was found that at $\tau_L=4$, the initial condition Eq. (B13) was reproduced with an accuracy of 1 part in 10^6. This accuracy was obtained using truncated matrix representations of $\cos(\mathbf{W}^{1/2}t_0)$ and $\mathbf{W}^{\pm1/2}\sin(\mathbf{W}^{1/2}t_0)$ which were accurate to one part in 10^8. The total number of iterations with these matrices was 60.

Plots of the reduced local temperature vs τ_L for the cases $L=10$ and $L=25$ for the same crystals show the same general features. There is an abrupt fall-off at $\tau_L=1$, and there is a considerable spread among the cooling curves for $\tau_L>1$. However, one noteworthy difference between the cooling curves for the perfect and disordered crystals is apparent when the cooling curves for the cases $L=10$, 15, and 25 are compared on the τ_L time scale. The cooling curves for the perfect crystal practically coincide in the three cases, $L=10$, 15, and 25, whereas the cooling curves for any one of the disordered crystals do not. The magnitude of the differences is illustrated in Fig. 5, where the three cooling curves for the perfect crystals and the three for disordered crystal #14 are plotted. Disordered crystal #14 is typical in the sense that similar plots for the other disordered lattices show both larger and smaller differences.

The calculations for the same mass distributions considered in Fig. 4 with a mass ratio $m_2/m_1=5/4$ have been repeated for the mass ratio $m_2/m_1=2$. The results for the reduced local temperature in the middle of the hot region, with $L=15$ are plotted as a function of τ_L in Fig. 6. As in the previous case, the cooling curve for the perfect monatomic crystal composed of particles with the harmonic mean mass $\bar{m}$ is indicated by open circles. The increase in the mass ratio from 5/4 to 2 has the effect of enhancing the differences among the disordered crystal cooling curves and between the disordered crystal and monatomic crystal cooling curves noted in the $m_2/m_1=5/4$ case. It is to be expected that in the limit in which the number of particles in the crystal and in the hot region are very large, differences between cooling curves for different random isotope arrangements will be negligible. Even though the time required for the generation of a random mass distribution and the calculation of the cooling curves for $L=10$, 15, and 25 is only 2 minutes in the case of a 100-particle crystal, it is not now feasible to verify this expectation.

The principal conclusions which can be drawn from these numerical experiments are that a significant fraction of the energy in the hot region propagates away at the speed of sound of the regular diatomic crystal and that the tail of the temperature-time curve for a disordered crystal decreases more slowly than that for the perfect crystal in which the sound speed is the

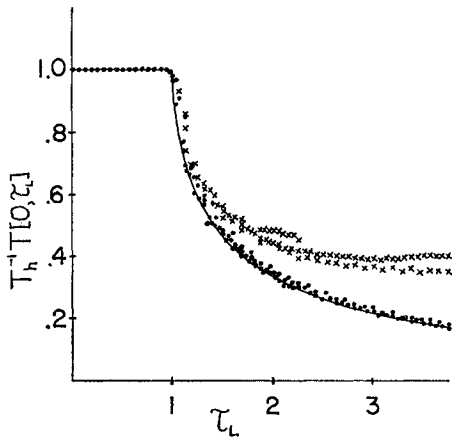

FIG. 5. The reduced local temperature denoted by crosses is plotted as a function of τ_L in the case of random mass distribution #14 for a hot region consisting of 21, 31, and 51 particles ($L=10$, 15, and 25) when $m_2=(5/4)m_1$. The corresponding reduced local temperature denoted by dots is plotted as a function of τ_L in the case of the 100-particle monatomic crystal with $\bar{m}=(10/9)m_1$. The solid curve represents the analytic result, Eq. (B25).

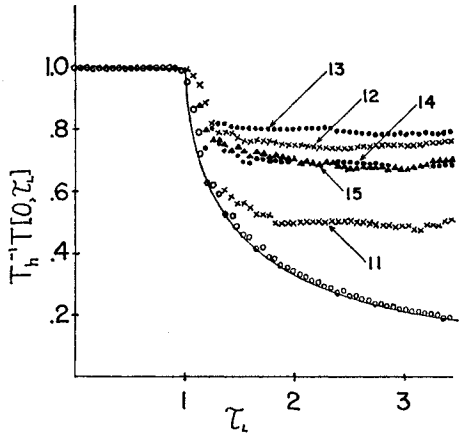

FIG. 6. The reduced local temperature in the middle of a hot region is plotted as a function of τ_L for the five isotopically disordered 100-particle crystals considered in Fig. 4. In the present case $m_2=2m_1$ and $L=15$. The corresponding reduced local temperature is plotted for a perfect crystal (open circles) consisting of 100 particles with the harmonic mean mass $\bar{m}=(4/3)m_1$. The solid curve represents the analytic result for the perfect crystal, Eq. (B25).

same. The precise nature of the decay law for $T_h^{-1}\times T[0,\tau_L]$ in an isotopically disordered infinite crystal when $L\gg 1$ is of particular interest, but remains to be determined.

SUMMARY

In Sec. A we treated the problem of obtaining the momentum autocorrelation function of a lattice particle in a system in thermal equilibrium; and in Sec. B we treated an energy transport problem in terms of the time dependence of the ensemble average kinetic energy of a lattice particle in a spatially nonuniform ensemble. As a consequence of the linearity of the equations of motion, it was possible in each case to solve the problem formally for an arbitrary mass distribution and lattice structure. Furthermore, a relation was established in each case between the statistical property of interest and the solution of the same initial value problem of the lattice equations of motion, Eq. (A8) or Eq. (B13). The formal solutions were studied in detail for a series of infinite, one-dimensional crystals with nearest neighbor interactions: (1) the perfect crystal, (2) the one-defect crystal, and (3) the isotopically disordered crystal.

In Sec. A, explicit analytic expressions were obtained for the momentum autocorrelation function of particles in a perfect and a one-defect crystal. In addition, in the one-defect crystal, the quantum-mechanical momentum autocorrelation function of a very heavy defect particle was studied. In the case of the isotopically disordered crystal, an identity was established between the average momentum autocorrelation function of all the lattice particles and the frequency spectrum of the crystal.

In Sec. B, explicit analytic solutions of the energy-transport problem were obtained for the perfect and the one-defect crystal. Numerical solutions were presented for a set of five different isotopically disordered 100-particle crystals.

ACKNOWLEDGMENTS

I wish to thank the following persons: Dr. H. Oser for suggesting the particular method of calculation used in determining the cooling curves for the disordered crystals and for supervising the calculations; Dr. F. W. J. Olver for an advance copy of his manuscript which proved to be extremely useful in the calculations in Sec. B1 and B2; and Professor E. Teramoto for a preprint describing his work on the energy transport problem.

APPENDIX I: DETERMINATION OF THE TIME DEPENDENCE OF THE MOMENTUM AUTOCORRELATION FUNCTION WHEN $\mathcal{Q}\gg\phi$

The expression for the quantum-mechanical momentum autocorrelation function is

$$r_{00}(t)=\mathrm{Re}\{\langle \mathfrak{p}[0,t']\mathfrak{p}[0,t'+t]\rangle\}/\langle \mathfrak{p}^2[0,t']\rangle$$
$$=\langle \mathfrak{p}^2[0,t']\rangle^{-1}k_BTM$$
$$\times\frac{\mathcal{Q}+1}{2\pi i}\int_{\mathfrak{C}}\frac{\phi z\cot(\phi z)}{\mathcal{Q}z+(z^2+1)^{1/2}}\exp(\omega_0 tz)dz. \quad (I.1)$$

In estimating the time dependence of $r_{00}(t)$ when $\mathcal{Q}\gg\phi$ and $\mathcal{Q}\gg 1$, we distinguish two cases: $0\leqslant\phi\leqslant\pi/2$ and $\pi/2<\phi\ll\mathcal{Q}$. In the first case $0\leqslant\phi\leqslant\pi/2$, the method used in estimating the classical momentum autocorrelation function[3] can be used directly; and in the second case $\pi/2<\phi\ll\mathcal{Q}$, a slight modification is necessary.

First Case: $0\leqslant\phi\leqslant\pi/2$

This case includes the classical limit $\phi=0$ where the factor $\phi z\cot(\phi z)$ is equal to unity and Eq. (I.1) for $r_{00}(t)$ is identical with the expression for $\rho_{00}(t)$ in Eq. (A26)

$$\rho_{00}(t)=\langle p^2[0,t']\rangle^{-1}k_BTM\frac{\mathcal{Q}+1}{2\pi i}\int_{\mathfrak{C}}\frac{\exp(\omega_0 tz)}{\mathcal{Q}z+(z^2+1)^{1/2}}dz. \quad (I.2)$$

In this classical limit, the integral appearing in Eq. (I.2) is transformed by replacing the vertical cut connecting $+i$ and $-i$ by a semicircular cut in the left half plane connecting $+i$ and $-i$ (see Fig. 7a). In the process, a pole of $\{\mathcal{Q}z+(z^2+1)^{1/2}\}^{-1}$ at $z=-(\mathcal{Q}^2-1)^{-1/2}\doteq-\mathcal{Q}^{-1}$ is uncovered. The integral in Eq. (I.2) can then be expressed as the sum of two quantities: the residue of the integrand at the pole $z=-(\mathcal{Q}^2-1)^{-1/2}$ and the line integral around the semicircular cut. In the classical limit when $\mathcal{Q}\gg 1$, it is easy to show[3] that the magnitude of the integral around the cut is less than $\sqrt{2}\mathcal{Q}^{-1}$. Consequently, a very precise estimate of the classical mo-

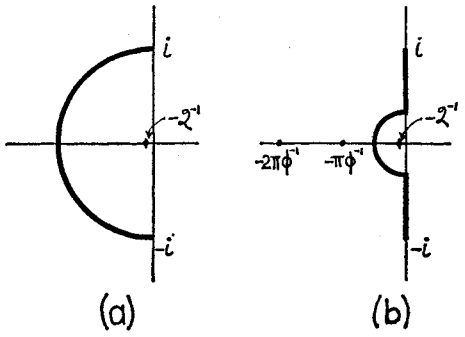

FIG. 7. (a) The form of the cut used in estimating the classical momentum autocorrelation function $\rho_{00}(t)$. (b) The form of the cut used in estimating the quantum-mechanical autocorrelation function $r_{00}(t)$ for ϕ in the interval $\pi/2<\phi\ll\mathcal{Q}$.

mentum autocorrelation function is obtained, namely,

$$\rho_{00}(t)=\exp(-\mathcal{Q}^{-1}\omega_0 t)+\delta(t)\,, \tag{I.3}$$

where $|\delta(t)|\leqslant\sqrt{2}\mathcal{Q}^{-1}$.

For all values of ϕ in the range $0\leqslant\phi\leqslant\pi/2$, the same arguments used in evaluating the integral in Eq. (I.2) can be used for $r_{00}(t)$ in Eq. (I.1). The residue of the integrand in Eq. (I.1) at $z=-(\mathcal{Q}^2-1)^{-1/2}$ can be expressed as $\exp(-\mathcal{Q}^{-1}\omega_0 t)+\delta_1(t)$, where $|\delta_1(t)|<c\mathcal{Q}^{-1}$; and an upper bound of the integral around the cut, $\delta_2(t)$, is $|\delta_2(t)|<\sqrt{2}(\phi\coth\phi)\mathcal{Q}^{-1}$. Therefore, in the case $0\leqslant\phi\leqslant\pi/2$, for $\mathcal{Q}\gg1$

$$r_{00}(t)=\exp(-\mathcal{Q}^{-1}\omega_0 t)+\delta(t)\,, \tag{I.4}$$

where $|\delta(t)|<c\mathcal{Q}^{-1}$.

Second Case: $\pi/2<\phi\ll\mathcal{Q}$

The function $\phi z\cot(\phi z)$ has poles at $z=\pm\pi\phi^{-1}$, $\pm2\pi\phi^{-1}\cdots$; and for values of ϕ in the range $\pi<\phi\ll\mathcal{Q}$, there is at least one of these poles inside the semicircular cut shown in Fig. 7(a). To avoid this complication, we use the cut shown in Fig. 7(b). This cut consists of a semicircular portion whose radius is $\frac{1}{2}\pi\phi^{-1}$ and two vertical segments connecting $+i$ and $-i$. The transformed expression for the quantum-mechanical autocorrelation function of the heavy particle is the sum of two quantities

$$r_{00}(t)=\langle p^2[0,t']\rangle^{-1}k_BTM\left\{\frac{\mathcal{Q}+1}{\mathcal{Q}-\mathcal{Q}^{-1}}\phi(\mathcal{Q}^2-1)^{-1/2}\right.$$
$$\times\cot[\phi(\mathcal{Q}^2-1)^{-1/2}]\exp[-\omega_0(\mathcal{Q}^2-1)^{-1/2}t]$$
$$\left.+\frac{\mathcal{Q}+1}{2\pi i}\int_{\mathcal{C}'}\frac{\phi z\cot(\phi z)}{\mathcal{Q}z+(z^2+1)^{1/2}}\exp(\omega_0 tz)dz\right\}. \tag{I.5}$$

The first term in braces in Eq. (I.5) is the residue of the integrand at $z=-(\mathcal{Q}^2-1)^{-1/2}$ and the second term is the line integral around the cut shown in Fig. 7(b). In the present case where $\mathcal{Q}\gg\phi>\pi/2$, the residue can be expressed as

$$\frac{\mathcal{Q}+1}{\mathcal{Q}-\mathcal{Q}^{-1}}\phi(\mathcal{Q}^2-1)^{-1/2}$$
$$\times\cot[\phi(\mathcal{Q}^2-1)^{-1/2}]\exp[-\omega_0(\mathcal{Q}^2-1)^{-1/2}t]$$
$$=\exp[-\mathcal{Q}^{-1}\omega_0 t]+\delta_1(t)\,, \tag{I.6}$$

where $|\delta_1(t)|<c_1\phi\mathcal{Q}^{-1}$ and c_1 is of order unity.

Next, consider the problem of estimating the contour integral in Eq. (I.5). It splits into two parts; and each part is equal to the difference of two line integrals along opposite sides of a portion of the cut

$$\frac{\mathcal{Q}+1}{2\pi i}\int_{\mathcal{C}'}\frac{\phi z\cot(\phi z)}{\mathcal{Q}z+(z^2+1)^{1/2}}\exp(\omega_0 tz)dz$$
$$=2\frac{\mathcal{Q}+1}{\pi}\int_{\frac{1}{2}\pi\phi^{-1}}^{1}\frac{\phi y\coth(\phi y)}{(\mathcal{Q}^2-1)y^2+1}(1-y^2)^{1/2}\cos(\omega_0 ty)dy$$
$$+\frac{\mathcal{Q}+1}{\pi}\int_{3\pi/2}^{\pi/2}\frac{\frac{1}{2}\pi\cot(\frac{1}{2}\pi e^{i\theta})}{(\mathcal{Q}^2-1)\frac{1}{4}\phi^{-2}\pi^2e^{2i\theta}-1}[1+\tfrac{1}{4}\pi^2\phi^{-2}e^{2i\theta}]^{1/2}$$
$$\times\exp[2i\theta+\tfrac{1}{2}\pi\phi^{-1}\omega_0 te^{i\theta}]\tfrac{1}{2}\pi\phi^{-1}d\theta\,. \tag{I.7}$$

The first integral on the right in Eq. (I.7) $\mathcal{I}_1(t)$, which represents the contribution from the vertical portions of the cut, satisfies the following inequality

$$|\mathcal{I}_1(t)|<2\pi^{-1}(\mathcal{Q}+1)\phi\coth(\pi/2)[1-\tfrac{1}{4}\pi^2\phi^{-2}]^{1/2}$$
$$\times\int_{\frac{1}{2}\pi\phi^{-1}}^{1}y[(\mathcal{Q}^2-1)y^2+1]^{-1}dy$$
$$<\pi^{-1}\frac{\phi}{\mathcal{Q}-1}\coth(\pi/2)[1-\tfrac{1}{4}\pi^2\phi^{-2}]^{1/2}$$
$$\times\left\{\ln\left(\frac{4\phi^2}{\pi^2}\right)-\ln\left[1+\frac{4\phi^2\pi^{-2}-1}{\mathcal{Q}^2}\right]\right\}. \tag{I.8}$$

In the present case where $\mathcal{Q}\gg\phi$, a simpler (and weaker) version of the inequality in Eq. (I.8) is

$$|\mathcal{I}_1(t)|<\coth(\pi/2)\left[\frac{2\phi}{\pi}\ln\frac{2\phi}{\pi}\right]\mathcal{Q}^{-1}. \tag{I.9}$$

The second integral on the right in Eq. (I.9), $\mathcal{I}_2(t)$, which represents the contribution from the semicircular portion of the cut, satisfies the inequality

$$|\mathcal{I}_2(t)|<(\mathcal{Q}+1)\frac{\pi^2}{4\phi}[1+\tfrac{1}{4}\pi^2\phi^{-2}]^{1/2}\coth(\pi/2)$$
$$\times[\tfrac{1}{4}(\mathcal{Q}^2-1)\pi^2\phi^{-2}-1]^{-1}$$
$$<[1+\tfrac{1}{4}\pi^2\phi^{-2}]^{1/2}\coth(\pi/2)\phi\mathcal{Q}^{-1}.\quad\text{For }\mathcal{Q}\gg\phi \tag{I.10}$$

We now combine the estimates in Eqs. (I.6), (I.9), and (I.10), substitute them in Eq. (I.5), and obtain the following estimate of the quantum-mechanical momentum autocorrelation function for ϕ in the range $\mathcal{Q}\gg\phi>\pi/2$:

$$r_{00}(t)=\exp(-\mathcal{Q}^{-1}\omega_0 t)+\delta(t), \tag{I.11}$$

where $|\delta(t)|<c(\phi\ln\phi)\mathcal{Q}^{-1}$.

APPENDIX II: DETERMINATION OF THE TIME DEPENDENCE OF THE ZERO-TEMPERATURE MOMENTUM AUTOCORRELATION FUNCTION FOR $\mathcal{Q}\gg1$

The integral in Eq. (A53) can be written as

$$\int_0^1 \frac{y(1-y^2)^{1/2}}{y^2+\mathcal{Q}^{-2}}\cos(\omega_0 t y)dy$$
$$=\int_0^1 \frac{y\cos(\omega_0 t y)}{y^2+\mathcal{Q}^{-2}}dy+\int_0^1 y^{-1}[(1-y^2)^{1/2}-1]$$
$$\times\cos(\omega_0 t y)dy+\int_0^1 \frac{\mathcal{Q}^{-2}y\cos(\omega_0 t y)}{(y^2+\mathcal{Q}^{-2})[1+(1-y^2)^{1/2}]}dy. \tag{II.1}$$

This decomposition of the original integral into the sum of three integrals is advantageous when $\mathcal{Q}\gg1$ because the last integral, $I_3(t)$, is negligible compared to the first two, $I_1(t)$ and $I_2(t)$, and because the explicit time dependence of $I_1(t)$ and $I_2(t)$ can be determined. An upper bound for $I_3(t)$ is

$$|I_3(t)|=\left|\int_0^1 \frac{\mathcal{Q}^{-2}y\cos(\omega_0 y t)}{(y^2+\mathcal{Q}^{-2})[1+(1-y^2)^{1/2}]}dy\right|$$
$$<\mathcal{Q}^{-2}\int_0^1 y(y^2+\mathcal{Q}^{-2})^{-1}dy<\mathcal{Q}^{-2}\ln(\mathcal{Q}^2+1).$$

Therefore, Eq. (II.1) is equivalent to

$$\int_0^1 y(1-y^2)^{1/2}(y^2+\mathcal{Q}^{-2})^{-1}\cos(\omega_0 t y)dy\doteq I_1(t)+I_2(t).$$

The integral $I_1(t)$ can be expressed in terms of the exponential integral $E_1(z)=\int_z^\infty u^{-1}e^{-u}du$ as

$$I_1(t)=\int_0^1 y(y^2+\mathcal{Q}^{-2})^{-1}\cos(\omega_0 t y)dy$$
$$=\tfrac{1}{2}\exp(\mathcal{Q}^{-1}\omega_0 t)E_1(\mathcal{Q}^{-1}\omega_0 t)+\tfrac{1}{4}\exp(-\mathcal{Q}^{-1}\omega_0 t)$$
$$\times[E_1(\mathcal{Q}^{-1}\omega_0 t e^{-i\pi})+E_1(\mathcal{Q}^{-1}\omega_0 t e^{i\pi})]$$
$$-\tfrac{1}{4}\exp(-\mathcal{Q}^{-1}\omega_0 t)[E_1(-i\omega_0 t-\mathcal{Q}^{-1}\omega_0 t)$$
$$+E_1(i\omega_0 t-\mathcal{Q}^{-1}\omega_0 t)]-\tfrac{1}{4}\exp(\mathcal{Q}^{-1}\omega_0 t)$$
$$\times[E_1(-i\omega_0 t+\mathcal{Q}^{-1}\omega_0 t)+E_1(i\omega_0 t+\mathcal{Q}^{-1}\omega_0 t)]. \tag{II.2}$$

The function $E_1(z)$ is defined so that $E_1(z)$ is real on the positive real z axis, and a cut extends from $z=0$ to $z=-\infty$ on the negative real axis.

The integral $I_2(t)$ is equal to [50]

$$I_2(t)=\int_0^1 y^{-1}[(1-y^2)^{1/2}-1]\cos(\omega_0 t y)dy$$
$$=\int_0^1 y^{-1}[(1-y^2)^{1/2}-1]dy$$
$$-\int_0^{\omega_0 t}\left\{\int_0^1[(1-y^2)^{1/2}-1]\sin(y\sigma)dy\right\}d\sigma$$
$$=\ln 2-1-\frac{\pi}{2}\left[\int_0^{\omega_0 t}\mathbf{H}_0(\sigma)d\sigma-\mathbf{H}_1(\omega_0 t)\right]$$
$$-\int_0^{\omega_0 t}[\cos\sigma-1]\frac{d\sigma}{\sigma}, \tag{II.3}$$

where $\mathbf{H}_n(\ )$ is a Struve function. Although we have succeeded in evaluating the integrals $I_1(t)$ and $I_2(t)$, Eqs. (II.2) and (II.3), their explicit dependence upon the time is not obvious. There are two time scales evident in Eq. (II.2) for $I_1(t)$, $t=\omega_0^{-1}$ and $t=\mathcal{Q}\omega_0^{-1}$; and there are different approximate expressions for $I_1(t)$ and $I_2(t)$ depending upon the value of the time relative to these two time scales. In the remainder of this Appendix we will obtain approximate expressions for $I_1(t)$ and $I_2(t)$ which are valid in the time intervals: $0\leqslant t\ll\omega_0^{-1}$; $0.1\omega_0^{-1}\leqslant t\leqslant 10\omega_0^{-1}$; $t\gg\omega_0^{-1}$ but $t\ll\mathcal{Q}\omega_0^{-1}$; $0.01\mathcal{Q}\omega_0^{-1}\leqslant t\leqslant 100\mathcal{Q}\omega_0^{-1}$; and $t>100\mathcal{Q}\omega_0^{-1}$.

Approximate Expressions for $I_1(t)$

The integral $I_1(t)$ has been expressed in terms of the exponential integral $E_1(z)$ in Eq. (II.2). The following convergent series expansion and asymptotic series for $E_1(z)$ will be used [51]:

$$E_1(z)=-\gamma-\ln z-\sum_{n=1}^{\infty}\frac{(-z)^n}{n!n} \tag{II.4}$$

$$E_1(z)\sim z^{-1}e^{-z}\sum_{m=0}m!(-z)^{-m}. \tag{II.5}$$

On the negative real z axis, the above series take the form

$$E_1(xe^{\pm\pi i})=\mp i\pi-\gamma-\ln x-\sum_{n=1}^{\infty}\frac{x^n}{n!n},\quad x>0 \tag{II.6}$$

and

$$E_1(xe^{\pm\pi i})\sim\mp i\pi-x^{-1}e^{-x}\sum_{m=0}m!x^{-m},\quad x>0. \tag{II.7}$$

---

[50] Ref. 34, p. 69.

[51] A. Erdelyi, W. Magnus, F. Oberhettinger, and F. G. Tricomi, *Higher Transcendental Functions* (McGraw-Hill Book Company, Inc., New York, 1953), Vol. 2, Sec. 9.7.

When $t \ll \omega_0^{-1}$, the expression for $I_1(t)$ reduces to

$$I_1(t) \cong \ln \mathcal{Q} + \cdots . \tag{II.8}$$

When $t \sim \omega_0^{-1}$, the expression for $I_1(t)$ is

$$I_1(t) \cong -\gamma - \ln(\mathcal{Q}^{-1}\omega_0 t) - \mathrm{Re}\{E_1(-i\omega_0 t)\} . \tag{II.9}$$

Values of $\mathrm{Re}\{E_1(-i\omega_0 t)\}$ can be obtained from tables.[52]

When $t \gg \omega_0^{-1}$ but $t \ll \mathcal{Q}\omega_0^{-1}$ ($\mathcal{Q}^{-1}\omega_0 t$ is still small compared to one), the approximate expression for $I_1(t)$ obtained from Eq. (II.9) is

$$I_1(t) \cong -\gamma - \ln(\mathcal{Q}^{-1}\omega_0 t) + (\omega_0 t)^{-1} \sin(\omega_0 t) . \tag{II.10}$$

In the range $0.01\ \mathcal{Q}\omega_0^{-1} < t < 100\mathcal{Q}\omega_0^{-1}$, the expression for $I_1(t)$ is

$$I_1(t) \cong \tfrac{1}{2} \exp(\mathcal{Q}^{-1}\omega_0 t) E_1(\mathcal{Q}^{-1}\omega_0 t) + \tfrac{1}{2} \exp(-\mathcal{Q}^{-1}\omega_0 t) \times \mathrm{Re}\{E_1(\mathcal{Q}^{-1}\omega_0 t e^{-i\pi})\} + (\omega_0 t)^{-1} \sin \omega_0 t . \tag{II.11}$$

Useful numerical tables of the combination of exponentials and exponential integrals in Eq. (II.11) are given by Miller and Hurst.[53] The last term in Eq. (II.11) is very small compared to the first two terms in our application, $\mathcal{Q} \gg 1$.

Finally, when $t \gg \mathcal{Q}\omega_0^{-1}$, the expression for $I_1(t)$ is

$$I_1(t) \cong -(\mathcal{Q}^{-1}\omega_0 t)^{-2} . \tag{II.12}$$

Approximate Expressions for $I_2(t)$

When $t \ll \omega_0^{-1}$, the expression for $I_2(t)$, Eq. (II.3), reduces to

$$I_2(t) \cong \ln 2 - 1 .$$

In the interval $0.1\omega_0^{-1} \leqslant t \leqslant 10\omega_0^{-1}$, a more convenient expression for $I_2(t)$ can be obtained by replacing $-\int_0^{\omega_0 t}(1-\cos\sigma)\sigma^{-1}d\sigma$ by[54]

$$\gamma + \ln(\omega_0 t) + \mathrm{Re}\{E_1(-i\omega_0 t)\} . \tag{II.13}$$

Upon substituting Eq. (II.13) in Eq. (II.3), one obtains

$$I_2(t) = \ln 2 - 1 + \gamma + \ln(\omega_0 t) + \mathrm{Re}\{E_1(-i\omega_0 t)\} - \frac{\pi}{2}\left\{\int_0^{\omega_0 t} \mathbf{H}_0(\sigma)d\sigma - \mathbf{H}_1(\omega_0 t)\right\} . \tag{II.14}$$

In the interval $0.1\omega_0^{-1} \leqslant t \leqslant 10\omega_0^{-1}$, tables of numerical values of all the functions in Eq. (II.14) are available.[55]

In the range $t > 10\omega_0^{-1}$ where values of $\int_0^{\omega_0 t}\mathbf{H}_0(\sigma)d\sigma$ are not tabulated, a more useful expression than Eq. (II.13) can be derived for $I_2(t)$. From Eq. (II.3), the original form of $I_2(t)$, one can obtain

$$I_2(t) = \int_0^1 y^{-1}[(1-y^2)^{1/2} - 1]\cos(\omega_0 t y)\, dy = -\int_0^1 \frac{y\cos(\omega_0 t y)}{(1-y^2)^{1/2}+1} dy . \tag{II.15}$$

After integrating Eq. (II.15) by parts and after some rearranging to isolate the singular factor $(1-y^2)^{-1/2}$ which is introduced, one obtains

$$I_2(t) = -\frac{\sin(\omega_0 t)}{\omega_0 t} + (\omega_0 t)^{-1}\int_0^1 (1-y^2)^{-1/2}\sin(\omega_0 t y)dy - (\omega_0 t)^{-1}\int_0^1 [1+(1-y^2)^{1/2}]^{-1}\sin(\omega_0 t y)dy . \tag{II.16}$$

The first integral on the right in Eq. (II.16) can be evaluated.[56] The procedure of integrating by parts and isolating the singular factor can be repeated twice more starting with the second integral on the right in Eq. (II.16). The final result is

$$I_2(t) = (1+\omega_0^{-2}t^{-2})^{-1}\left\{-\frac{\sin(\omega_0 t)}{\omega_0 t} + \frac{\cos(\omega_0 t)}{\omega_0^2 t^2} + \frac{\sin(\omega_0 t)}{\omega_0^3 t^3} - \frac{\frac{1}{2}}{\omega_0^2 t^2} + \left(\frac{1}{\omega_0 t} - \frac{2}{\omega_0^3 t^3}\right)\frac{\pi}{2}\mathbf{H}_0(\omega_0 t) - \frac{1}{\omega_0^2 t^2}\left[1 - \frac{\pi}{2}\mathbf{H}_1(\omega_0 t)\right]\right\} + \Delta(t) , \tag{II.17}$$

where the magnitude of the last term $\Delta(t)$ in Eq. (II.17) is less than $8\omega_0^{-4}t^{-4}$.

APPENDIX III: EVALUATION OF THE REDUCED LOCAL TEMPERATURE IN A PERFECT LATTICE

The expression for the reduced local temperature given in Eq. (B24) is

$$T_h^{-1}T[0,\tau_L] = J_0^2(2L\tau_L) + 2\sum_{l=1}^{2L} J_l^2\left(l\frac{2L}{l}\tau_L\right) . \tag{B24}$$

In evaluating the sum in Eq. (B24), we make use of a uniform asymptotic expansion of Bessel functions (with error estimates) which has been developed by Olver.[46,47] The expansion is

$$J_l(lx) \sim l^{-1/3}\phi(\zeta)\{\mathrm{Ai}(l^{2/3}\zeta)[1 + \sum_{s=1}^{r} l^{-2s}A_s(\zeta)] + l^{-4/3}\mathrm{Ai}'(l^{2/3}\zeta)\sum_{s=0}^{r-1} l^{-2s}B_s(\zeta)\} , \tag{III.1}$$

---

[52] *Tables of the Exponential Integral for Complex Arguments*, National Bureau of Standards Applied Mathematics Series (U. S. Government Printing Office, Washington, D. C., 1958), Vol. 51.

[53] J. Miller and R. P. Hurst, Math. Tables Aids Computation, **12**, 187 (1959).

[54] Ref. 51, Vol. 2, Sec. 9.8.

[55] G. N. Watson, *A Treatise on the Theory of Bessel Functions* (The University Press, Cambridge, England, 1944), 2nd ed., p. 752; and M. Abramowitz, J. Math. Phys. **29**, 49 (1950).

[56] Ref. 34, p. 69.

where

$$\zeta=\begin{cases}\left\{\frac{3}{2}\ln\left(\dfrac{1+(1-x^2)^{1/2}}{x}\right)-\frac{3}{2}(1-x^2)^{1/2}\right\}^{2/3}, & \\ \qquad 0<x\leqslant 1 \quad \text{(III.2)} & \\ -\{\frac{3}{2}(x^2-1)^{1/2}-\frac{3}{2}\sec^{-1}x\}^{2/3}, \quad x\geqslant 1 \quad \text{(III.3)}\end{cases}$$

and

$$\phi(\zeta)=[4\zeta(1-x^2)^{-1}]^{1/4}. \qquad \text{(III.4)}$$

$\mathrm{Ai}(x)$ and $\mathrm{Ai}'(x)$ denote the Airy integral and its derivative[57]

$$\mathrm{Ai}(x)=\pi^{-1}\int_0^\infty \cos(\tfrac{1}{3}t^3+xt)dt,$$

and the functions $A_s(\zeta)$ and $B_s(\zeta)$ are defined by recurrence relations.[46] The recurrence relations are

$$B_s(\zeta)=\tfrac{1}{2}\zeta^{-1/2}\int_0^\zeta \zeta^{-1/2}\{F(\zeta)A_s(\zeta)-A_s''(\zeta)\}d\zeta$$

and

$$A_{s+1}(\zeta)=-\tfrac{1}{2}B_s'(\zeta)+\tfrac{1}{2}\int F(\zeta)B_s(\zeta)d\zeta,$$

where

$$A_0(\zeta)=1$$

$$F(\zeta)=\frac{5}{16\zeta^2}+\frac{\zeta}{4}\frac{x^2(x^2+4)}{4(x^2-1)^3},$$

and $x=x(\zeta)$ is defined implicitly by Eqs. (III.2) and (III.3). When $x\geqslant 1$, the expressions for $B_0(\zeta)$ and $A_1(\zeta)$ are

$$B_0(\zeta)=\frac{3\tau_1+5\tau_1^3}{24\zeta_1^{1/2}}-\frac{5}{48\zeta_1^2}$$

and

$$A_1(\zeta)=-\frac{81\tau_1^2+462\tau_1^4+385\tau_1^6}{1152}-\frac{7(3\tau_1+5\tau_1^3)}{1152\zeta_1^{3/2}}+\frac{455}{4608\zeta_1^3},$$

where $\zeta_1=-\zeta$ and $\tau_1=(x^2-1)^{-1/2}$.

Olver has shown[47] that if terms up to and including $l^{-4}B_2(\zeta)$ and $l^{-6}A_3(\zeta)$ are retained in Eq. (III.1), then the remainder or error term is less than one unit in the 8th significant figure when $l\geqslant 8$. Consequently, in the sum in Eq. (B24) from $l=8$ to $2L$, $J_l[l(2L/l)\tau_L]$ can be replaced by Eq. (III.1) with $r=3$. For $\tau_L>1$, the sum of the terms in Eq. (B24), which are not included in $\sum_{l=8}^{2L}$, is negligible (of order L^{-1}). The Airy functions introduced into Eq. (B24) have the argument

$$l^{2/3}\zeta=-\left\{\tfrac{3}{2}l\int_1^{2L\tau_L/l}(x^2-1)^{1/2}x^{-1}dx\right\}^{2/3}$$

$$=-(2L)^{2/3}\left\{\frac{3}{2}\left(\tau_L^2-\frac{l^2}{4L^2}\right)^{1/2}-\frac{3}{2}\frac{l}{2L}\sec^{-1}\left(\frac{2L}{l}\tau_L\right)\right\}^{2/3}.$$

For τ_L not too close to unity, $-l^{2/3}\zeta$ is large ($\sim L^{2/3}$) for all values of l, $l\leqslant 2L$. Consequently, all of the functions $\mathrm{Ai}(l^{2/3}\zeta)$ and $\mathrm{Ai}'(l^{2/3}\zeta)$ can be replaced by their asymptotic formulas, for large negative arguments.[57]

$$\mathrm{Ai}(l^{2/3}\zeta)\sim\pi^{-1/2}(-l^{2/3}\zeta)^{-1/4}\cos\left[-\frac{\pi}{4}+2L\left\{\left(\tau_L^2-\frac{l^2}{4L^2}\right)^{1/2}-\frac{l}{2L}\sec^{-1}\left(\frac{2L}{l}\tau_L\right)\right\}\right] \qquad \text{(III.5)}$$

and

$$\mathrm{Ai}'(l^{2/3}\zeta)\sim\pi^{-1/2}(-l^{2/3}\zeta)^{1/4}\sin\left[-\frac{\pi}{4}+2L\left\{\left(\tau_L^2-\frac{l^2}{4L^2}\right)^{1/2}-\frac{l}{2L}\sec^{-1}\left(\frac{2L}{l}\tau_L\right)\right\}\right]. \qquad \text{(III.6)}$$

The use of these asymptotic formulas for every l, $8\leqslant l\leqslant 2L$, is justified if $\frac{2}{3}(l^{2/3}|\zeta|)^{3/2}$ is large compared to one, i.e.,

$$l\int_1^{2L\tau_L/l}(x^2-1)^{1/2}x^{-1}dx\gg 1 \qquad \text{(III.7)}$$

or

$$2L\left\{\left(\tau_L^2-\frac{l^2}{4L^2}\right)^{1/2}-\frac{l}{2L}\sec^{-1}\left(\frac{2L}{l}\tau_L\right)\right\}\gg 1. \qquad \text{(III.8)}$$

The condition expressed in Eqs. (III.7) and (III.8) is clearly satisfied, except when τ_L is close to 1 and, at the same time, l is close to $2L$. We can determine the lower limit of τ_L such that the inequality in Eq. (III.7) is satisfied over the whole range of values of l, from the condition

$$2L\int_1^{\tau_L}(x^2-1)^{1/2}x^{-1}dx\geqslant(2L)^{1/2}, \qquad \text{(III.9)}$$

where $(2L)^{1/2}$ is assumed to be large. Because the integral in Eq. (III.9) is greater than $2^{3/2}(\tau_L-1)^{3/2}/3\tau_L$, the inequality in Eq. (III.9) is satisfied if $\tau_L-1>2^{-1}3^{2/3}\times(2L)^{-1/3}$. Thus, except for a very small time interval $1<\tau_L<1+(2L)^{-1/3}$, the asymptotic formulas in Eqs. (III.5) and (III.6) can be used.

Substituting these asymptotic formulas and the definition of $\phi(\zeta)$, Eq. (III.4), in Eq. (III.1) for $J_l[l(2L/l)\tau_L]$, one obtains

$$J_l\left(l\frac{2L}{l}\tau_L\right)\sim(2L)^{-1/2}(2/\pi)^{1/2}(\tau_L^2-y^2)^{-1/4}\left\{\cos\left[2L(\tau_L^2-y^2)^{1/2}-2Ly\sec^{-1}(y^{-1}\tau_L)-\frac{\pi}{4}\right]\left[1+\sum_{s=1}^{3}(2Ly)^{-2s}A_s(\zeta)\right]+\sin\left[2L(\tau_L^2-y^2)^{1/2}-2Ly\sec^{-1}(y^{-1}\tau_L)-\frac{\pi}{4}\right]\times\left[\sum_{s=0}^{2}(2Ly)^{-2s-1}(-\zeta)^{1/2}B_s(\zeta)\right]\right\}, \qquad \text{(III.10)}$$

[57] J. C. P. Miller, *The Airy Integral*, British Association for the Advancement of Science, Mathematical Tables (The University Press, Cambridge, England, 1946), Part-Vol. B.

where the variable $y=l/2L$ ranges from $8/2L$ to 1. There is a final simplification of the expression for $J_l(ly^{-1}\tau_L)$ in Eq. (III.10) which depends upon the properties of $(2Ly)^{-2s}A_s(\zeta)$, $s\geqslant 1$ and $(-\zeta)^{1/2}(2Ly)^{-2s-1}\times B_s(\zeta)$, $s\geqslant 0$. These terms constitute corrections to the leading term in the asymptotic series and were retained in order to have a uniform accuracy of one part in 10^8 for Bessel functions of all orders between $l=8$ and $l=2L$, independent of the value of $2L\tau_L l^{-1}$. In the present application, the magnitudes of these additional terms are negligible for all values of l, $8\leqslant l\leqslant 2L$, for one of two reasons. Either the factors $(2Ly)^{-2s}$ are negligible or the coefficients $A_s[\zeta(y)]$, $s\geqslant 1$ and $[-\zeta(y)]^{1/2}B_s[\zeta(y)]$, $s\geqslant 0$ are negligible.

These assertions concerning the magnitudes of $A_s[\zeta(y)]$, $s\geqslant 1$ and $[-\zeta(y)]^{1/2}B_s[\zeta(y)]$, $s\geqslant 0$ can be verified as follows. When $x\geqslant 1$ or $2L\tau_L l^{-1}\geqslant 1$, and $\zeta=-\{\frac{3}{2}[(2L/l)^2\tau_L{}^2-1]^{1/2}-\frac{3}{2}\sec^{-1}[(2L/l)\tau_L]\}^{2/3}$, the expression for $(2Ly)^{-2}A_1(\zeta)$ is[47]

$$(2Ly)^{-2}A_1(\zeta)=(2Ly)^{-2}\left\{-\frac{81\left[\left(\frac{2L}{l}\tau_L\right)^2-1\right]^{-1}+462\left[\left(\frac{2L}{l}\tau_L\right)^2-1\right]^{-2}+385\left[\left(\frac{2L}{l}\tau_L\right)^2-1\right]^{-3}}{1152}\right.$$
$$\left.-\frac{7\left\{3\left[\left(\frac{2L}{l}\tau_L\right)^2-1\right]^{-1/2}+5\left[\left(\frac{2L}{l}\tau_L\right)^2-1\right]^{-3/2}\right\}}{1152(-\zeta)^{3/2}}+\frac{455}{4608}(-\zeta)^{-3}\right\}$$
$$=(2L)^{-2}\left\{-\frac{81[\tau_L{}^2-y^2]^{-1}+462y^2[\tau_L{}^2-y^2]^{-2}+385y^4[\tau_L{}^2-y^2]^{-3}}{1152}\right.$$
$$\left.-\frac{7\{3[\tau_L{}^2-y^2]^{-1/2}+5y^2[\tau_L{}^2-y^2]^{-3/2}\}}{1728\{[\tau_L{}^2-y^2]^{1/2}-y\sec^{-1}(y^{-1}\tau_L)\}}+\frac{455}{4608}\left(\frac{4}{9}\right)\{[\tau_L{}^2-y^2]^{1/2}-y\sec^{-1}(y^{-1}\tau_L)\}^{-2}\right\}. \quad \text{(III.11)}$$

In Eq. (III.11) the largest term (i.e., the one with the most singular dependence on $[\tau_L{}^2-y^2]^{-1}$ is $-(2L)^{-2}y^4\times(385/1152)(\tau_L{}^2-y^2)^{-3}$. In the most unfavorable circumstance, when $\tau_L=1+(2L)^{-1/3}$ and $y=1$, this term is equal to

$$(2L)^{-2}\frac{385}{1152}[2(2L)^{-1/3}+(2L)^{-2/3}]^{-3}=\frac{(2L)^{-1}}{4}\frac{385}{1152}[1+\tfrac{1}{2}(2L)^{-1/3}]^{-3}.$$

It can be shown that the other terms in Eq. (III.11) are also negligible for $L\gg 1$ and $\tau_L>1+(2L)^{-1/3}$; and the same arguments lead to a similar result for the higher order terms, $(2Ly)^{-2s}A_s(\zeta)$.

The expression for $(2Ly)^{-1}(-\zeta)^{1/2}B_0(\zeta)$ is[47]

$$(2Ly)^{-1}(-\zeta)^{1/2}B_0(\zeta)=(2Ly)^{-1}(-\zeta)^{1/2}\left\{\frac{3\left[\left(\frac{2L}{l}\tau_L\right)^2-1\right]^{-1/2}+5\left[\left(\frac{2L}{l}\tau_L\right)^2-1\right]^{-3/2}}{24(-\zeta)^{1/2}}-\frac{5}{48(-\zeta)^2}\right\}$$
$$=(2L)^{-1}\frac{1}{24}\left\{3[\tau_L{}^2-y^2]^{-1/2}+5y^2[\tau_L{}^2-y^2]^{-3/2}-\frac{\frac{5}{3}}{(\tau_L{}^2-y^2)^{1/2}-y\sec^{-1}(y^{-1}\tau_L)}\right\}. \quad \text{(III.12)}$$

For all $\tau_L>1+(2L)^{-1/3}$ and for all y, $0\leqslant y\leqslant 1$, it can be shown from Eq. (III.12) that when $2L\gg 1$,

$$(2Ly)^{-1}(-\zeta)^{1/2}B_0(\zeta)<(5/96)L^{-1/2}.$$

Similar results can be obtained for the higher order terms $(2Ly)^{-2s-1}(-\zeta)^{1/2}B_s(\zeta)$.

As a consequence of the above estimates of the magnitudes of $A_s[\zeta(y)]$, $s\geqslant 1$ and $[-\zeta(y)]^{1/2}B_s[\zeta(y)]$, $s\geqslant 0$ the asymptotic expression for $J_l[l(2L/l)\tau_L]$ for $\tau_L>1+(2L)^{-1/3}$, $8\leqslant l\leqslant 2L$ and $2L\gg 1$, is

$$J_l\left(l\frac{2L}{l}\tau_L\right)\sim(2L)^{-1/2}\left(\frac{2}{\pi}\right)^{1/2}(\tau_L{}^2-y^2)^{-1/4}$$
$$\times\cos\left[2L\mu(\tau_L,y)-\frac{\pi}{4}\right], \quad \text{(III.13)}$$

where $\mu(\tau_L,y)=(\tau_L{}^2-y^2)^{1/2}-y\sec^{-1}(y^{-1}\tau_L)$. It is clear

that upon inserting this result in Eq. (B24) for the reduced local temperature the summation over l, $(2L)^{-1}\sum_{l=8}^{2L}$, can be replaced by an integration over y, $\int_{8/2L}^{1}dy$; and the result is

$$T_h^{-1}T[0,\tau_L]=\frac{4}{\pi}\int_{8/2L}^{1}\frac{\cos^2[2L\mu(\tau_L,y)-\pi/4]}{(\tau_L^2-y^2)^{1/2}}dy$$
$$=\frac{2}{\pi}\int_{8/2L}^{1}\frac{1+\cos[4L\mu(\tau_L,y)-\pi/2]}{(\tau_L^2-y^2)^{1/2}}dy. \quad \text{(III.14)}$$

Furthermore, in the limit of very large values of $2L$ and for $\tau_L>1+(2L)^{-1/3}$, the integral in Eq. (III.14) which involves $\cos[4L\mu(\tau_L,y)-\pi/2]$ can be neglected compared to the first term. The value of the reduced local temperature obtained from Eq. (III.14) is

$$T_h^{-1}T[0,\tau_L]=(2/\pi)\sin^{-1}(1/\tau_L), \quad \text{for} \quad \tau_L>1+(2L)^{-1/3}, \quad \text{(III.15)}$$

a result which becomes exact in the limit $2L\to\infty$. The simplest method for obtaining the corresponding value of $T_h^{-1}T[0,\tau_L]$ for $\tau_L<1$ is to make use of the identity expressed in Eq. (B23),

$$T_h^{-1}T[0,\tau_L]=1-2\sum_{l=2L+1}^{\infty}J_l^2\left(\frac{2L}{l}\tau_L\right). \quad \text{(III.16)}$$

In the sum on the right-hand side of Eq. (III.16), the parameter $(2L/l)\tau_L$ is always less than one if $\tau_L<1$. In this case, the asymptotic approximation, Eq. (III.1), for $J_l[l(2L/l)\tau_L]$ is

$$J_l\left(\frac{2L}{l}\tau_L\right)\sim l^{-1/3}\left(\frac{4\zeta}{1-4L^2\tau_L^{-2}l^{-2}}\right)^{1/4}\mathrm{Ai}(l^{2/3}\zeta), \quad \text{(III.17)}$$

where

$$\zeta=\left\{\tfrac{3}{2}\int_{2L\tau_L l^{-1}}^{1}(1-x^2)^{1/2}x^{-1}dx\right\}^{2/3}. \quad \text{(III.18)}$$

The argument of the Airy function $l^{2/3}\zeta$ is positive and large for all terms in Eq. (III.16) if $\tau_L<1-(2L)^{-1/3}$. This last condition on τ_L can be obtained in the same way that the condition $\tau_L>1+(2L)^{-1/3}$ was obtained. Replacing $Ai(l^{2/3}\zeta)$ by its asymptotic formula, the expression for $J_l[l(2L/l)\tau_L]$ becomes

$$J_l\left(\frac{2L}{l}\tau_L\right)\sim(2L)^{-1/2}(2\pi)^{-1/2}\left(\frac{l^2}{4L^2}-\tau_L^2\right)^{-1/4}\times\exp\{-\tfrac{2}{3}l\zeta^{3/2}\}, \quad \text{(III.19)}$$

for $l\gtrsim 2L$ and $\tau_L<1-(2L)^{-1/3}$. Inserting this expression for $J_l[l(2L/l)\tau_L]$ in Eq. (III.16), the reduced local temperature is

$$T_h^{-1}T[0,\tau_L]=1-\pi^{-1}\sum_{l=2L+1}^{\infty}(l^2-4L^2\tau_L^2)^{-1/2}\times\exp\{-\tfrac{4}{3}l\zeta^{3/2}\}, \quad \text{(III.20)}$$

for $\tau_L<1-(2L)^{-1/3}$. The sum in Eq. (III.20) can be shown to be negligible in the following way. A term-by-term upper bound on

$$S=\sum_{l=2L+1}^{\infty}(l^2-4L^2\tau_L^2)^{-1/2}\exp\{-\tfrac{4}{3}l\zeta^{3/2}\}$$

is

$$S\leqslant(2L)^{-1}(1-\tau_L^2)^{-1/2}\times\sum_{l=2L+1}^{\infty}\exp\left\{-2l\int_{\tau_L}^{1}(1-x^2)^{1/2}x^{-1}dx\right\}$$
$$\leqslant(2L)^{-1}(1-\tau_L^2)^{-1/2}\sum_{l=2L+1}^{\infty}\exp\{-\tfrac{1}{3}2^{5/2}l(1-\tau_L)^{3/2}\}$$
$$\leqslant(2L)^{-1}(1-\tau_L^2)^{-1/2}\frac{\exp\{-\tfrac{1}{3}2^{5/2}(2L+1)(1-\tau_L)^{3/2}}{1-\exp\{-\tfrac{1}{3}2^{5/2}(1-\tau_L)^{3/2}\}}. \quad \text{(III.21)}$$

Even in the most unfavorable case, i.e., when $\tau_L=1-(2L)^{-1/3}$, the upper bound in Eq. (III.21) is

$$3\cdot 2^{-5/2}(2L)^{-1/3}\exp\{-\tfrac{1}{3}2^{5/2}(2L)^{1/2}\}.$$

We now summarize the result for the reduced local temperature in the middle of an initially hot region of a perfect, infinite, one-dimensional lattice consisting of a very large number of particles, $2L$,

$$T_h^{-1}T[0,\tau_L]=\begin{cases}1, & \text{if } \tau_L<1-(2L)^{-1/3}\\ (2/\pi)\sin^{-1}(1/\tau_L), & \text{if } \tau_L>1+(2L)^{-1/3}.\end{cases} \quad \text{(III.22)}$$